

**CYTOTOXIC EFFECTS OF
COBALT METAL IONS ON
OSTEOBLASTS: ARE
CALCIUM CHANNELS
INVOLVED?**

Sarah Wiseman BSc

**This Thesis is submitted in part fulfilment for the degree of
Masters of Science in Biomedical Engineering**

August 2012

Department of Bioengineering

Declaration of Authenticity and Authors Rights

This thesis is the result of the author's original research. It has been composed by the author and has not been previously submitted for examination which has led to the award of a degree.

The copyright of this thesis belongs to the author under the terms of the United Kingdom Copyright Acts as qualified by the University of Strathclyde Regulation 3.50. Due acknowledgement must always be made of the use of any material contained in, or derived from, this thesis.

Signed:

Date:

Acknowledgements

First and foremost, I would like to sincerely thank my supervisor, Professor M.H. Grant for all her support throughout the duration of this project. Without her guidance, motivation and endless knowledge, there would certainly be no thesis.

I would also like to thank Katie Handerson for her endless help during the experimentation phase; for answering all my questions and assisting me with anything and everything lab-related. Thanks also to Christopher Hamilton and Olga Posada for all their help with the confocal microscope, and any other assistance they may have provided in the lab.

Above all, and as ever, I would like to express my deepest gratitude to my family. To my parents, for the love, encouragement and every kind of support possible, that they have always shown me, but especially over the course of this Masters Degree. And to my brothers for keeping the bar impossibly high. Thanks to my friends, both at home and overseas, for being very willing to take my mind off my thesis, if only for a short time. And especially for Ruth and David; for the inspirational messages.

Abstract

Metal on Metal (MM) hip replacement implants have become a popular alternative to traditional metal on polyethylene (MP) devices due to their improved wear profiles and reduced associated risk of dislocation, wear debris and subsequent osteolysis. MM articulations are most commonly made of cobalt-chromium alloy and are associated with elevated levels of cobalt and chromium ions locally and systemically which may have detrimental effects on patients, including to their bone health.

Osteoblasts are a type of bone cell vital to overall bone function and turnover, and cobalt ions have been seen to inhibit osteoblast function by reducing alkaline phosphatase activity, calcium deposition and increasing chemokine secretion in osteoblasts, which may result in local osteolysis. These toxic effects of cobalt on osteoblasts may potentially arise due to metal ions entering tissue via calcium channels, and the aim of this project was to try to elucidate whether this theory was correct. The effects of acute exposure to cobalt on OST 5 cells, a rat osteoblast cell line, *in vitro*, were measured and calcium channel blockers were used in a bid to prevent cobalt-induced toxicity seen in cells, which if successful, would suggest the involvement of calcium channels in cobalt uptake.

Cobalt concentrations ranged from 0.1 – 200 μM , and nifedipine and verapamil were expected to block calcium channels at a concentration of 10 μM . Cell viability was assessed using neutral red and MTT assays. Cobalt was seen to significantly reduce OST 5 cell viability in a dose dependent manner, and though significant differences were seen in cobalt-treated and cobalt and verapamil-treated OST 5 cells, this calcium channel blocker did not significantly prevent cobalt-induced toxicity according to the results seen here. Further research must be conducted to definitively conclude whether or not calcium channels are involved in the uptake of cobalt ions into osteoblasts.

Contents

1. INTRODUCTION.....	1
1.1. Hip Joint.....	1
1.1.1. Hip Replacement.....	1
1.1.1.1. History of Hip Replacement.....	2
1.1.1.2. Modern Process.....	2
1.1.2. Hip Resurfacing.....	3
1.1.3. Materials Used in Hip Replacement.....	4
1.1.4. Risks and Complications.....	5
1.2. Medical Device Alerts Regarding MM Hip Implants.....	6
1.3. Cobalt.....	8
1.3.1. Cobalt Levels in Body Fluids.....	9
1.3.2. Metal Toxicity.....	10
1.3.3. Apoptosis.....	11
1.3.4. Immunological Effects of Cobalt.....	12
1.3.4.1. Macrophages and Chemokines.....	12
1.3.4.2. Lymphocytes.....	13
1.3.5. Pseudotumours.....	13
1.3.6. Infection.....	15
1.3.7. Systemic Effects.....	16
1.3.7.1. Canada Beer Drinkers Cardiomyopathy.....	17
1.3.7.2. Case Studies of Systemic Toxicity.....	18
1.3.8. Neurological Effects.....	20
1.4. Osteoblasts.....	21
1.4.1. Cobalt and Osteoblasts.....	22
1.5. Calcium Channels.....	24
1.5.1. Calcium Channels and Osteoblasts.....	25
1.5.2. Calcium Channel Blockers.....	26
1.5.2.1. Nifedipine and Verapamil.....	26
1.6. Aim of Project.....	27
2. MATERIALS AND METHODS.....	29
2.1. OST 5 Cells.....	30
2.1.1. Medium Preparation.....	30
2.1.2. Passaging Cells.....	30
2.1.3. Counting Cells.....	31

2.2.	Cobalt Concentrations.....	33
2.3.	Nifedipine Concentrations.....	33
2.4.	Verapamil Concentrations.....	33
2.5.	Administration to OST 5 Cells.....	34
2.6.	Viability Assays.....	39
2.6.1.	PBS.....	39
2.6.2.	Neutral Red.....	39
2.6.3.	MTT.....	40
2.7.	Confocal Microscopy.....	40
2.7.1.	Staining for Actin Using Phalloidin-FITC.....	41
2.7.2.	Cell Viability Staining Using Propidium Iodide and CFDA.....	42
2.8.	Statistics.....	43
3.	RESULTS.....	45
3.1.	Effect of Cobalt on OST 5 Cell Viability.....	45
3.2.	Effect of Nifedipine on OST 5 Cell Viability.....	49
3.2.1.	Nifedipine.....	49
3.2.2.	Nifedipine and Cobalt (100 μ M fixed).....	51
3.3.	Effect of Verapamil on OST 5 Cell Viability.....	53
3.3.1.	Verapamil	53
3.3.2.	Verapamil and Cobalt (100 μ M fixed).....	54
3.3.3.	Verapamil (10 μ M fixed) and Cobalt.....	56
3.4.	Osteoblast Images.....	60
3.4.1.	Unstained OST 5 Cells.....	60
3.4.2.	Phalloidin-FITC Stained OST 5 Cells.....	61
3.4.3.	Propidium Iodide and CFDA Stained OST 5 Cells	62
4.	DISCUSSION.....	64
4.1.	Are Calcium Channels Involved?.....	67
4.2.	Alternative Materials in THA.....	69
4.2.1.	Ceramics.....	69
4.2.2.	Titanium.....	70
4.3.	What's Next for Cobalt-Chromium in THA?.....	70
4.3.1.	Infection Control.....	71
	REFERENCES.....	73

1.Introduction

1.1. Hip Joint

The hip joint is a congruous, synovial ball-and-socket joint formed by the articulation of the spherical femur head and the cup-like acetabulum of the pelvis. It forms the primary connection between the bones of the lower limb and pelvis. Its primary function is supporting the body, in both dynamic and static postures, and is the most important joint in retaining balance. The femoral head is held in the acetabulum by various ligaments, and the articulating joint surfaces are covered by a strong, lubricated layer of hyaline cartilage, which cushions compressive forces and lubricates the joint. The acetabulum forms at the union of three bones; the ilium, pubis and ischium. The femur head is attached to the shaft by a thin neck region often prone to fracture in the elderly, mainly due to the degenerative effects of osteoporosis. Various muscles act on the joint, including the hamstring, adductor muscles and abductor muscles, to facilitate movement, and as the joint is congruous, rotation occurs in all directions.

1.1.1. Hip Replacement

Hip replacement refers to a medical procedure in which one or more sections of the hip joint are replaced by synthetic implants, and is the most successful, inexpensive and safest form of joint replacement surgery. Total hip arthroplasty (THA) involves replacing the acetabulum and femoral head, and is generally conducted to treat pain or joint failure caused by osteoarthritis, a joint disorder due to aging and wear-and-tear on the hip. The operation aims to reduce pain and improve overall hip function, and though it is the most common joint replacement surgery, patient satisfaction, both short and long-term, varies greatly.

1.1.1.1. History of Hip Replacement

Hip replacement dates back to 1891, when German Professor T. Gluck attempted replacement of the femoral head with ivory and nickel-plated screws (1). The first metallic hip replacement was performed by American Dr. Austin T. Moore in 1940 at Johns Hopkins hospital using a cobalt-chrome alloy, 'Vitallium' (1, 2), to replace the femur. During the 1940s steel and chrome artificial hips became more widespread, but were prone to loosening and wear. A later version of Moore's prosthesis using a fenestrated stem to allow bone ingrowth and longer-term attachment was introduced in 1952, and is still currently in use (1).

1.1.1.2. Modern Process

In 1962, Sir John Charnley designed a cemented, low friction arthroplasty joint consisting of a metal femoral head and stem articulated with a polyethylene acetabular component, both lubricated with synovial fluid. Due to its lack of friction, this design yielded excellent clinical results and was instrumental in the development of the modern artificial hip joint and had almost completely replaced previous designs by the 1970s (3). The cemented Exeter device was also developed during this era in the UK. However, early implants had the potential to loosen, become painful and cause bone erosion, which prompted searches for alternative methods. In recent times, there have been several evolutionary improvements made in the procedure and prostheses of THA. Ceramic is being introduced as an implant material in the place of polyethylene, due to reported reductions in joint wear. Metal-on-metal (MM) implants are also gaining popularity for this same reason, as they have been shown to reduce the need for revision of the acetabular component.

1.1.2. Hip Resurfacing

Hip resurfacing (HR) is an alternative to total hip arthroplasty (THA) where only the articulating surfaces of the joint are replaced (4); the femoral head is coated with a cylindrical metal cap and the acetabulum is replaced just as in a THA (5). Developed in the mid 1990's, especially for younger, physically active patients (6), resurfacing offers several advantages over THA; including the preservation of bone stock, if a revision should ever be needed (4), the elimination of the problem of femoral shaft loosening, restoration of normal joint mechanics (7, 8), reduced stress-shieldings (8, 9) and superior wear properties (10, 11). Revision of a modern resurfacing procedure is claimed to be less problematic than that of THA, in terms of operation time, blood loss and functional results (5), an advantage with younger patients who may outlive the predicted lifespan of their hip implants. Ball *et al*, 2007, found the results of metal-on-metal hip resurfacing (MM HR) to THA conversion comparable to primary THA in terms of surgical effort, safety and clinical outcome (10).

The first generation HR with metal-on-polyethylene (MP) bearing couples were implanted in the 1970s and early 1980s, but poor clinical results were yielded (12, 13). The introduction of metal-on-metal (MM) articulation renewed the interest in HR due to the potential of MM prostheses to survive over 20 year with low wear and no osteolysis incidence (14-16). MM THA and MMHR have become the most commonly used UK procedures in treating osteoarthritis in patients less than 60 years of age (17, 18). HR has shown encouraging short-term reports with a low incidence of failure, even after the resumption of high-level activities (17, 19, 20). Ten year success rates of hip resurfacing from studies in England report success equal to or greater than standard THA. In the US, the first modern resurfacing device received FDA approval in May 2006, while some 90 000 resurfacings have been performed world-wide. However, according to the National Joint Register for England and Wales in 2008, the three year revision rate for HR was 4.4% compared to 1.3% for cemented THA (www.njrcentre.org.uk), and the Australian Arthroplasty Register also reported a higher three year revision rate for hip resurfacing than for THA (3.1% v 2.1%) (www.dmac.adelaide.edu/au.aonjrr) (21).

1.1.3. Materials used in Hip Replacement

THA has greatly improved the quality of life of patients suffering from traumatic/degenerative joint diseases, but first generation polyethylene prostheses released significant amounts of wear particles through friction at the bearing interface. This was a major concern for the longevity of these THA (22), as these polyethylene wear particles have been cited as a main source of osteolysis (23-25). In an attempt to circumvent polyethylene-induced osteolysis and improve implant longevity, the orthopaedic industry developed articulations producing minimal amounts of wear particles (26-29). Ceramic-on-ceramic (CC) bearings offer high wear-resistance, low wear and low noise friction and unanticipated bearing fracture (30); highly cross linked polyethylene bearing reduce wear of polyethylene (31), but long-term clinical results are not yet available. There has been a resurgence in MM arthroplasty, due to their low volumetric wear in hip simulators (32, 33) and in clinical practice (14), which results in significantly less wear debris and subsequent peri-prosthetic osteolysis (34-36). As a result, many MM implants used over the last two decades are still functioning in patients who received implants at a young age (37). MM bearings are commonly used among young patients, whose life expectancy is greater than that of traditional elderly hip replacement patients, and where longevity is particularly important. Extended durability of the hip replacement and a reduction in the need for revision are anticipated with MM arthroplasty (38, 39). 45% of hip replacements are in men less than 54 years old in the UK (40). Though the use of MM bearings eliminate, or substantially reduce the need for polyethylene bearings, concern has been expressed about the increased particulate and ionic metal generation (39), and the biological implications of these metal species. Titanium alloys have been shown to have limitations as articulating surfaces and should not be considered for wear couples in THR due to significant wear being shown (38). Cobalt and chromium alloy has shown reasonable wear and corrosion profiles and continues to be evaluated, in a bid to overcome wear debris-related issues.

1.1.4. Risks and Complications

Risks and complications are similar to those associated with all joint replacements – including femoral neck fracture (41, 42), dislocation, loosening (43), impingement (44), infection, osteolysis, metal sensitivity, nerve palsy, pain and death. Andrews *et al*, 2011, cites the most common adverse events necessitating revision after MM THA as early prosthetic fracture, the failure of osseo-integration of the prosthesis which results in aseptic loosening, unexplained pain and inflammatory masses (21, 45-49). According to Queally *et al*, 2009, the leading cause of arthroplasty implant



Figure 1.1: X-ray of implanted DePuy ASR™ XL MM acetabular hip system prosthesis from Mao *et al*, 2011.

failure is wear debris-mediated osteolysis with associated aseptic loosening (50-52). ~10% of primary THA require revision 10 years after the initial procedure (51, 53).

Smith *et al*, 2012, carried out an analysis of the National Joint Registry of England and Wales for primary hip replacements between 2003 and 2011; 31 171 of the 402 051 THA procedures carried out were stemmed MM, and these were found to fail at high rates. Larger heads failed earlier, 3.2% incidence of revision was seen for 28 mm and 5.1% for 52 mm heads at 5 years in men ages 60 years. In younger women, 5 year revision rates

were 6.1% for 46 mm MM devices compared with 1.6% for MP implants, and CC articulations were associated with improved survival by comparison. Failure rate statistics such as these have led to the recall of MM THA and HR devices in recent times (54)

1.2. Medical Device Alerts Regarding MM Hip Implants

In recent times, the subject of MM THA and HR has attracted a lot of attention in both the media and the medical world. Though previously believed to be at the forefront of progress in the area of hip prosthetics, the health hazards of these devices are beginning to be documented and reported, as the safety, well being and an improved quality of life must ultimately be the aspiration of the procedure.

In September 2010, the Medicines and Healthcare products Regulatory Agency (MHRA) released a medical device alert urging immediate action on the subject of DePuy ASR™ (articular surface replacement) MM hip replacement implants (MDA/2012/044), in which those involved in the implantation of these prostheses were instructed to cease the use of this particular model, return all unused models to the manufacturer, and inform all previous recipients of the DePuy ASR™ about the recall, and organise follow-up appointments for them. This particular system consisted of acetabular cups for resurfacing or replacement, surface replacement heads for resurfacing, and XL femoral heads for replacement. DePuy ASR™ hip implants have been used in the UK since 2003, and the main reason cited for the recall was the prostheses being associated with much higher rates of revision at 5 years than initially expected. At the British Hip Society annual conference in March 2011, some alarming figures were presented on MM devices, which displayed revision results similar to the withdrawn DePuy ASR™ implant. Research showed that 49% of DePuy ASR™ devices needed to be replaced within 6 years, and 12-15% of other MM hip devices required revision within 5 years. Pain was reported as the first symptom experienced by patients who eventually underwent implant revision, and X-rays depicting loosening along with elevated blood levels of chromium and cobalt ions were sometimes, but not always seen. MRI scans of cystic and/or solid masses and fluid collections were also reported.

In January 2012, an investigation was launched into MM hip implants by the media and several medical regulators due to the occurrence of elevated metal ion levels

seen in some MM implant patients and the potential dangers of these events. In the UK, media outlets such as the BBC and The Telegraph newspaper felt it was necessary to bring this issue to the attention of the public, as concerns were growing that risks from this device were beginning to appear much greater than previously thought, and Channel 4 news reported that over 30 000 people in the UK had received MM hip implants at this time. An MHRA statement released on the 30 January 2012 assured the threat posed by MM devices was low, with only an extreme minority experiencing serious problems, but further investigation and monitoring of evidence would be ongoing.

The most recent medical device alert at the time of this project was issued by the MHRA on the 25 June 2012, where updated advice for clinicians managing patients with several variations of MM hip implants was given (MDA/2012/036). Four different MM hip replacements were listed as carrying a risk; DePuy ASR™ hip replacements, MM hip resurfacing implants, MM total hip replacements with a head diameter ≥ 36 mm and also those with a head diameter of >36 mm. The main problem outlined in this warning was the development of soft tissue reactions seen in the minority of patients who had received one of these implants, caused by a reaction to metal wear particles leached from the implant, and the systemic risks carried by the entry of these metal particles into the bloodstream. As this will adversely affect revision surgery, extra vigilance is recommended in cases of poorly performing hip implants, as early revision is important. Follow-up recommendations are provided in this alert, in the areas of annual follow-up following implantation, appropriate imaging to visualise the prosthesis and whether it appears to have undergone corrosion, blood testing to assess blood metal ion levels, and situations where revision should be considered, in symptomatic and asymptomatic patients. Patients presenting with muscle or bone damage on MRI scans should be of utmost concern.

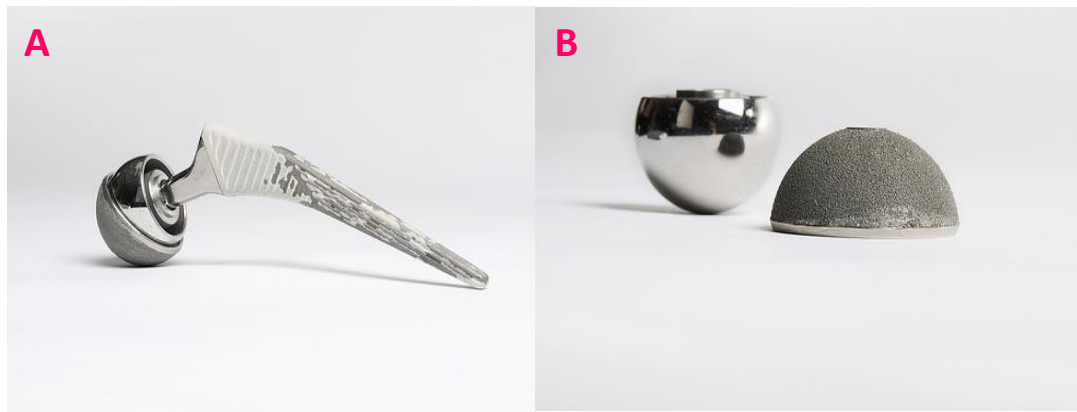


Figure 1.2: DePuy ASR™ hip cup and stem (A) and acetabulum cup and spherical femoral head (B). The cup surface is grainy in a bid to promote bone ingrowth.

1.3. Cobalt

This project focuses on the release of cobalt rather than chromium ions, and their potential toxic effects. Co^{2+} have been found to be more toxic than Cr^{3+} in a variety of settings in previous literature, including macrophages (55) and osteoblasts (50, 56), though Cr^{6+} is believed to be the form of ion in which the metal is released from orthopaedic implants, which has the potential to be more toxic than Co^{2+} and Cr^{3+} due to their smaller size. Higher circulating levels of cobalt ions (Co^{2+}) than chromium ions (Cr^{3+} and Cr^{6+}) have been recorded previously in MM THA and HR patients post-implantation, giving rise to the theory that cobalt levels could have more implication in the systemic adverse effects seen in these patients (57). One reported case of possible systemic toxicity following MM THA reported elevated cobalt serum levels, but no elevation in chromium serum levels (58). However, it should be noted that chromium levels can be found to be higher in some cases, e.g. plasma levels in Rizetti *et al*, 2009 (57).

Cobalt (Co; atomic number 27) naturally occurs in chemical combinations and was first isolated by George Brandt in the 1730's in Sweden by reductive smelting. The free element has the appearance of a hard, ductile, lustrous bluish-grey metal. It has high boiling and melting points (2870 °C and 1495 °C, respectively), and this

temperature stability makes its alloys suitable for use in parts for aircraft engines that require magnetic, high-strength and wear/corrosion resistant alloys; it is widely used in batteries and electroplating, due to its high resistance to oxidation; it is important commercially in its cobalt⁶⁰ isotope, which is used in the treatment of cancer and as a radioactive tracer. It is a useful gamma ray source as it can be produced in high activity and predictable quantities. Cobalt is also essential to many animals as a trace dietary mineral as it is a component of vitamin B₁₂. In inorganic form, it is also an active nutrient for algae, bacteria and fungi. The resistance of cobalt to wear and corrosion makes its alloys useful in orthopaedic implants. Cobalt-chromium alloys are currently used in prosthetic knee and hip implants (59), and cobalt alloys are also useful in dental alloys, for nickel allergy sufferers (60). Cobalt-chrome alloy in solid form is very well tolerated by the body, and previous literature states *in vivo* testing shows no pathological changes compatible with systemic toxicity (61).

1.3.1. Cobalt Levels in Body Fluids

Cobalt ions can be generated in the peri-prosthetic space due to electrochemical corrosion of metallic particles, or possibly as a result of phagocytosis of cobalt-chromium (CoCr) particles by cells and the exposure of particles to a series of oxidative mechanisms designed to destroy foreign bodies (62-64). Andrews *et al*, 2011, claims normal circulating physiological levels of cobalt and chromium to be <0.25 µg/L (0.005 µM), but following MM THA, elevated circulating levels of the metal ions can occur in hip synovial fluid and peripheral blood (21). Whole blood concentrations of cobalt ions (Co²⁺) can reach 4.6 µM (65), while local hip synovial fluid levels have been measured at 30 µM *in vivo* (66), which are higher than values of circulating total chromium ion levels, which have been recorded at 2.3 µM and 25 µM for blood and hip synovial fluid concentrations respectively (65, 66). Circulating levels of cobalt are usually highest in the first few months after implantation, but persistent elevation can occur as late as ten years post-surgery

(67). Toxicity caused by these metal ions locally (in the peri-prosthetic space) and systemically is a cause of concern for metal on metal implants (50, 68), potentially causing chromosomal changes (64, 69), hypersensitivity and instability (45, 70). There may also be complex issues present with the definitive collection and analysis of metal ion levels, as well as with the statistical methodologies and reporting of results and previous literature has shown a characteristic variability in these factors. (71). As MM THA is performed more and more frequently, manufacturing differences (clearance, roughness, metallurgy, head size, etc.) are apparently affecting performance. Modern MM bearings have uniformly shown higher levels of blood cobalt and chromium, the principal elements in CoCr alloy used in MM HR implants (72), when compared to pre-operative values, and in comparison to the levels in MP patients (19, 73-76). Engh *et al*, 2009, measured 2 year post-operative ion levels for 28 mm metal on polyethylene bearings compared with 28 and 36 mm metal on metal bearings. The MM cobalt serum, erythrocyte and urine ion levels were higher two years post-implantation than MP levels (77). Elevated cobalt ion levels are commonly seen in intermediate and long-term follow-up studies of MM arthroplasties (67), which have shown to be higher than levels associated with bearings of different materials (78). Despite satisfactory short-term implant survival, there is an increasing concern that CoCr alloy MM HR implants release a large amount of very small wear particles and metal ions (79).

1.3.2. Metal toxicity

Metal toxicity remains a concern (locally, in peri-prosthetic space, and systemically) (80-82). As previously mentioned, substantial levels of metallic products can be transferred into the host environment from a metallic device (83, 84). CoCr alloy is used for MM bearings, due to its wear performance profile, but cobalt and chromium ions are produced by mechanical wear and corrosion in the periprosthetic tissue as a result of MM articulation (85, 86). Cobalt and chromium constitute 90% of the CoCr alloy used in MM hip resurfacing implants (87), and

particles generated from these alloys have a size range in the nanometer scale (88). Although wear rates are lower in MM bearing surfaces, previous research has found that the amount of particles generated by these implants can be up to 500 times higher than the amount of micrometer sized particles from conventional MP bearings (20). Metal nanoparticles corrode to either produce a protective passive layer or dissolve into charged free ions (85). Cobalt and chromium ions have been detected in solution during metal alloy corrosion (89). However, other studies have found that MP bearings can generate 100 mm^3 500 nm particles per year, while MM implants can generate 1 mm^3 40 nm CoCr particles (17, 90). The vast range of metal ion generation reported in the literature is one reason why this area needs further attentions. These ions will eventually reach the blood circulation where metal ion concentration has shown to be significantly elevated ($>20 \text{ nM}$) in patients with MM THA (75, 91, 92). Periprosthetic tissues cobalt concentration measured in 6 patients 20 months post-implantation was found to be 1000-times higher than control patients (30mg/g vs. 0.03mg/g) (93). The toxicity of released cobalt ions from MM THA is a cause for concern (55, 56, 94, 95), but the role of these ions in physiopathology of MM THA infection and cytotoxicity has not yet been studied fully (96).

1.3.3. Apoptosis

Petit *et al*, 2004, analyzed the effects of cobalt and chromium ions on bcl-2, bax, caspase-3 and caspase-8 expression; these protein families play a central role in the modulation of apoptosis. Cobalt and chromium ions inhibited bcl-2 expression, stimulated bax and caspase-3 expression, and Cr ions stimulated caspase-8 expression also. Therefore, bcl-2 and caspase protein family expression is implicated in the induction of macrophage apoptosis, specifically the modulation of expression of these proteins (97). Cateles *et al*, 2001, analyzed the effects of Co^{2+} and Cr^{3+} ions on macrophages *in vitro*, by analyzing the implications of caspase-3 in the apoptotic pathway, with Co^{2+} and Cr^{3+} both inducing macrophage mortality in a dose-

dependent manner. Co^{2+} was found to be more toxic, inducing cell mortality up to 28% at 10 ppm, compared to 37% at 500 ppm Cr^{3+} (55). DNA fragmentation was induced by both ion types, but at a lower concentration of cobalt. The appearance of the caspase-3 active fragment is implicated in several apoptotic pathways. Cateles *et al*, 2003, looked at the effects of cobalt and chromium ions on macrophages in a more pro-longed incubation period (94). ELISA results confirmed that Co^{2+} and Cr^{3+} induced concentration and time-dependent increase of $\text{TNF-}\alpha$, a cytokine involved in systemic inflammation which has the ability to induce apoptotic cell death. Cell mortality increased as concentrations increased, especially at 48 hours. This study found that both Co^{2+} and Cr^{3+} induced macrophage apoptosis, measured by DNA analysis, with a stronger signal at 24 hours than 48 hours, suggesting the presence of more necrosis at 48 hours. A subsequent study which backed up this result evaluated cell death *in vitro* by transmission electron microscopy in addition to cell death detection ELISA, and also found non-inflammatory apoptosis predominant at 24 hours, and necrosis predominant at 48 hours at higher ion concentrations (98). However, the apoptotic effect of Cr^{6+} was not assessed in the above literature, which has also been found to cause apoptosis in macrophages (99).

1.3.4. Immunological Effects of Cobalt

1.3.4.1. Macrophages and Chemokines

The cytotoxic effects of cobalt ions have been demonstrated *in vitro* in macrophages, by induction of apoptosis and necrosis, $\text{TNF-}\alpha$ secretion and oxidation of proteins (50, 55, 94, 95, 97, 98). Cobalt has also previously been shown to enhance the *in vitro* secretion of IL-8 and MCP-1 in renal, gastric and colon epithelium, as well as monocytes and neutrophils (68), which shows the potent bioactivity of cobalt ions in a variety of cell types as well as their potential to induce a proinflammatory response. Products of metallic degradation may be transported from the site of implant and distributed systemically. Though the toxicological

importance of these trace metallic elevations remains to be elucidated, urine and serum metal concentrations may serve as useful tribological markers in the performance of MM *in vivo* (39). MM bearings are reported to release approximately three times more cobalt and chromium ions than MP hips (39, 100). Concern has been expressed that MP release ions that can cause DNA damage (64) and immune dysfunction, in the form of T-lymphocyte reduction (101), and threshold levels of blood cobalt and chromium were associated with reduced CD8+ T-cell counts (102) following implantation of a MM device. Hart *et al*, 2006, studied the relationship between metal ion levels and lymphocyte counts in patients with MM HR and found cobalt and chromium levels significantly elevated in patients with reduced lymphocyte numbers.

1.3.4.2. Lymphocytes

Elevated cobalt and chromium levels have previously been linked to lymphocytic DNA damage (103). In a pilot study, Hart *et al*, 2006, found lower peripheral lymphocyte counts in patients with MM hip replacements, compared to MP articulation patients (102). Hart *et al*, 2009, compared Co²⁺ and Cr³⁺ levels in whole blood and lymphocytes in patients with MM, CC and MP hip replacements, with the aim of elucidating whether higher metal ion levels were related to differences in lymphocyte counts. CD8+ and CD3+ lymphopenia was present in 15% and 13% of patients respectively with unilateral MM hips, and significant differences in absolute CD8+ lymphocyte subsets were seen in MM group in comparison to the other groups (104).

1.3.5. Pseudotumours

Concern has recently been expressed about soft-tissue reactions to metal wear debris, collectively called pseudotumours (46). These masses (tumours) may be cystic or solid ('pseudo'), and have been referred to as bursae (105), cysts (106) and inflammatory masses (107). These pseudotumours can appear with varying levels of

interference, from asymptomatic abnormality detected on a scan to a destructive lesion leading to revision of MM HR, and are associated with elevated cobalt and chromium serum levels (median Co^{2+} level - 3.8 $\mu\text{g/L}$ or 0.6 $\mu\text{M/L}$; total chromium level median – 11.5 $\mu\text{g/L}$ or 0.2 μM) (46). Hip aspirate cobalt and chromium levels have also shown to be higher (Co^{2+} – 701 $\mu\text{g/L}$ or 12 μM ; Cr^{3+} and Cr^{6+} – 329 $\mu\text{g/L}$ or 6 μM)(46). Occurrence of such reactions is rare, and precise prevalence remains unknown, but they are becoming increasingly reported (46, 65, 104, 108, 109). These reactions have previously been shown following MP THA (110, 111), and more recently following MM HR in Pandit *et al*, 2008, which included reports of bilateral pseudotumours in bilateral arthroplasties. In this study, pseudotumours were locally destructive, causing the need for revision in the majority of patients (46). Another series reported incidence of revision for pseudotumours at 8 years as being 0.5% in men, 5% in women over 40 years of age, and 25% in women less than 40 years of age (112); however, other long-term series have not reported high rates (113). Their histology has some features of aseptic-lymphocytic-vasculitic-associated lesions (ALVAL) (45), although they feature more marked necrosis. This histological feature is thought to represent a metal-induced systemic T-lymphocyte delayed (type IV) hypersensitivity reaction. This would partly explain the high prevalence in females, and bilateral appearance of pseudotumour, which is possibly related to previous exposure to jewellery. Based on these findings, delayed reaction to cobalt and chromium ions has been suggested to play a role in the aetiology of pseudotumours.

Grammatopoulos *et al*, 2009, aimed to determine the extent of the problem posed by pseudotumours by assessing the outcome of MM HR revised to conventional THA due to pseudotumour formation, which was previously claimed to yield good results (10, 114). Grammatopoulos states that outcome after revision of MM HR depends on indication for revision, and with indications other than inflammatory pseudotumours, the outcome was generally good and similar to primary THA. Outcome after revision for pseudotumour was poor with major complications occurring in ~50% of patients, with ~30% requiring further revision, and this study

recommended that patients presenting with symptomatic pseudotumours following MM HR should be given early revision to limit soft tissue damage (114). The effects on macrophages are also relevant here, due to the histological appearance of pseudotumours which are characterized by the presence of macrophages surrounding the extensive necrosis of the connective tissue, where metal particle clusters can also be found (46, 79). Additionally, macrophages are the dominant infiltrating cells that respond rapidly to biomaterial implantation in soft and hard tissue (115), and can act as antigen presenting cells in delayed hypersensitivity reactions driven by T lymphocytes (116). Kwon *et al*, 2009, investigated the potential cytotoxic effects of cobalt and chromium on Macrophage viability, observing dose dependent cytotoxic effects on macrophages *in vitro* with high concentrations of cobalt ions only. Based on the findings of this study, the cytotoxicity of high concentrations of metal nanoparticles phagocytosed by macrophages in the periprosthetic tissue may be an important factor in the pathogenesis of pseudotumours (79).

1.3.6. Infection

Infection following MM THA is a devastating complication, occurring in 1.5-2.5% of primary THA, and associated with a significant increase in hospitalization-related morbidity and mortality (96, 117). *Staphylococcus epidermis* is the most common etiological agent recovered from infected THA (118). Neutrophils, the first line of defence against infection, are potentially exposed to cobalt ions in the periprosthetic tissue by the wear of metal on metal THA. Neutrophils are most exposed to the potential effects of cobalt, as these innate immune cells are recruited during MM THA infections. While the toxicity of cobalt is still being debated, these ions potentially inhibit the Hv1 proton channel, which sustains superoxide production by neutrophils. This study shows how the antibacterial activity of human neutrophils can be altered by Co^{2+} *in vitro* by the inhibition of Hv1 proton channels; submillimolar concentrations of cobalt inhibit proton currents, impair cystolic acid

extrusion and decrease the production of superoxide. Thus, cobalt reduces the ability of human neutrophils to kill two strains of *S. Epidermis* by up to 7-fold at concentrations of 100 mM. By inhibiting proton channels, Co^{2+} released by metal prostheses may therefore promote bacterial infections in patients with MM THA (96).

1.3.7. Systemic Effects

The systemic effects of metal ions remain relatively unknown. Once generated in the periprosthetic space, cobalt ions bind to serum proteins (mainly albumin) and are transported systemically before being excreted by the renal and gastrointestinal systems (45, 55, 67, 78, 86). Elevated serum levels of cobalt have been demonstrated systemically, for which the clinical implications have not yet been elucidated (94, 97). High concentrations of cobalt chloride have been shown to be toxic to the heart and liver in mice (119). In the endocrine system, Co^{2+} can prevent the uptake of iodine into the hormone thyroxine by inhibiting the tyrosine iodinase enzyme, which can induce hypothyroidism (120). Cobalt ions can also influence oestrogen signalling, by binding to cellular oestrogen receptors (121). A 2007 review of toxic effects of orthopaedic metals listed chromium ions as having a greater effect systemically, than cobalt ions (122). Cr^{6+} can induce changes in haemoglobin and haematocrit values in blood (123); the ions can also cause hepatocellular necrosis with acute ingestion (124) and impair renal function when accumulated in epithelial kidney cells (125). Chronic Cr^{6+} exposure can cause detrimental effects to male fertility, including decreased sperm count and sperm abnormalities (126). The effect of both chromium and cobalt ions on the respiratory system has been documented due to occupational exposure, and include an increased incidence of asthma and inflammation (127). Increased levels of cobalt and chromium ions have been seen in cord blood of women who became pregnant following MM prosthesis implantation, suggesting metallic ions may translocate into foetal circulation (128).

1.3.7.1. Canada Beer Drinkers Cardiomyopathy

The story of Quebecs beer-drinkers cardiomyopathy began in August 1965, when the first patient was admitted to a Quebec hospital complaining of epigastric pain, localized to the upper abdomen. The patient was also short of breath, anxious, agitated and cyanotic, especially in the face, neck and abdomen. Cardiovascular examination revealed increased heartrate and low blood pressure. The patient admitted to regularly drinking ~25 pints of a certain beer a day, and was thus diagnosed with what doctors believed to be a rare form of alcoholic cardiomyopathy. He was given a large dose of thiamine, recovered slowly and went back to work (129).

Between August 1965 and April 1966, a total of 48 similar cases were seen in Quebec; 46 men and 2 women, ranging in ages from 25 to 66 (130). All patients were unusually heavy beer drinkers, with an average daily been intake of 24 pints per day, and over time it became apparent that the link between patients in this series was a preference for Brand XXX beer. This locally-brewed beer is popular in Quebec, and at the time of the incident commanded 80% of its market. Cobalt sulphate had been added to this beer in order to stabilize foam since July 1965 (129).

Most patients were in good health up until shortly, between one and 90 days, before admission (130). Gastrointestinal symptoms were the first to appear; nausea, vomiting and inability to intake food. Signs of heart failure appeared progressively; thoracic pain, dyspnea, ankle oedema, cyanosis, and a regular but rapid heartrate. This contrasted with other cardiomyopathies, where arrhythmias are common. Arterial emboli were seen in five cases, being the cause of death in two of these (129). Patients were given various different treatments; digitalis, diuretics, thiamine, anticoagulants, and corticosteroids, for the treatment of shock. 20 of the 48 patients died, mostly in shock, which was unresponsive to medication; 14 within 24 hours of admission, one died between 24 and 48 hours, and five more after 48 hours (130). There were striking elevations in serum enzymes, which correlated with central hepatic necrosis found in the end stages of the disease.

Immunological and virological studies were negative, as was the search for toxic substances, such as lead and arsenic (129).

Following discharge, all symptoms, cardiovascular or otherwise, had subsided, despite many patients failing to follow correct diet and medication regimens, and many returning to their previous drinking habits (129). The syndrome which appeared in Quebec between August 1965 and April 1966 was similar to one present in Omaha, Nebraska and Minneapolis, Minnesota (131). This study recommended experimental reproduction in animals, but believed the epidemiological, clinical and pathological evidence seen in Quebec was strong enough to establish cobalt as an essential causative factor in this syndrome, though as a similar syndrome had not been seen before 1965, despite cobalt previously being used in higher dosages than the dose present in Brand XXX beer, evidence indicates that other unknown factors may have been present which increased the susceptibility of the patients to the toxicity of cobalt (129).

1.3.7.2. Case Studies of Systemic Toxicology

Two case studies appear in an Australian journal regarding cobalt toxicity in patients who received ASR XL Acetabular Hip Systems by DePuy Orthopaedics (58). The first of which regards a 73 year old woman who, five years earlier, underwent a hip replacement due to osteoarthritis. She presented with neurological symptoms, including memory difficulties, depression and cognitive decline; a continuous metal taste in her mouth; severe headaches and weight loss. She also complained of mild groin pain, but no other hip-related symptoms. X-rays showed that the implant was well-fixed and correctly aligned, but displayed mild osteopaenia around the acetabular component. Her serum cobalt level was 410 nmol/L (reference range 0 – 20 nmol/L) and serum chromium level was 240 nmol/L (reference range 0 - 100 nmol/L). Four years post-implantation, the woman suffered a cerebrovascular episode, during which stroke-like symptoms occurred: headaches, disorientation and dizziness, nausea and vomiting, and a feeling of being off-balance. Difficulty in

remembering names and registering information (written and aural) were cited as particularly difficult. The original hip implant was performed in 2006, consisting of a large diameter CoCr metal cup and a large modular metal head on a titanium Corail stem. In March 2011, a revision total hip replacement was performed, due predominantly to the elevated metal concentration and the systemic symptoms, in which the metal cup was replaced with a polyethylene cemented cup, and the metal head was changed to a ceramic one. Cobalt concentrations of the turbid joint fluid were measured at 4218 nmol/L at the time of revision surgery, and cerebrospinal fluid showed a cobalt ion level of 9 nmol/L, confirming that the metal ions had crossed the blood brain barrier. At an eight week post-surgery follow up, the patient felt much improved. She reported greater energy and less fatigue, and the disappearance of the metallic taste in her mouth. She also had regained a normal appetite and had gained weight. The hip pain dissipated and her serum cobalt level dropped from 410 to 60 nmol/L.

The second case study featured in Mao *et al*, 2011, discussed a 60 year old male who presented with systemic symptoms at a 4 year follow up for a right total hip replacement, performed to treat pain and stiffness caused by osteoarthritis, and before which he enjoyed general good health. No hip symptoms were reported but marked bone loss around the acetabular component was seen by x-ray. Three years post-surgery, symptoms began to develop which increased steadily in severity, including painful muscle fatigue in limbs and cramps in hands and feet, dyspnoea and feeling faint during simple tasks, and the inability to climb a flight of stairs without needing to rest. Problems with remembering names and poor concentration was also noted and hypertension, which had been previously stable, became uncontrolled and required further medication. At this time, the patients serum cobalt level measured at 185 nmol/L, and subsequently remained elevated at between 213 and 258 nmol/L. Chromium levels were never elevated. A revision THR was performed in February 2011 due to systemic symptoms, and the metal head and cup were replaced with ceramic and polyethylene versions. There was no apparent localised tissue reaction of metal debris. A serum cobalt level of 258

nmol/L at time of revision surgery fell to 42 nmol/L in the eight weeks post surgery. At this follow up, the patient reported significant decrease in muscle pains, improved energy levels and exercise tolerance.

1.3.8. Neurological Effects

Rizetti *et al*, 2009, reports a case study in which a 58 year old patient suffered progressive visual and hearing loss, after a left hip arthroplasty, which was revised five years later due to rupture of the ceramic head (57). On admission, neurological examination showed impairment of cranial nerves II and VIII bilaterally and mild distal sensory-motor disturbances. Haematological, infectious, neoplastic, metabolic and immunological diseases were subsequently ruled out and the patient underwent various investigative procedures, and within 2 months, the patient was completely blind, severely deaf, wheelchair-bound (due to lower limb hyposthenia). As tests for immune-mediated processes remained negative, the case was referred to toxicology, where raised concentrations of cobalt and chromium were unexpectedly found in different biological samples:

Table 1.2: elevated cobalt and chromium levels in various body fluids, references figures in brackets, in a patient following MM THA in Rizetti *et al*, 2009.

	Total Cobalt Ions (µg/L)	Total Chromium Ions (µg/L)
24 hour urine collection	1187 (0.1 – 1.5)	510 (0.05 – 2.2)
Blood	549 (0.05 – 2.7)	54 (0.1 – 0.5)
Plasma	90 (0.1 – 0.6)	210 (0.1 – 0.5)
Cerebrospinal Fluid (CSF)	11.4 (0.05 – 0.15)	4.4 (0.01 – 0.2)

Chromium levels were much lower than cobalt levels in all cases except plasma. Cobalt-chromium poisoning due to metal wear debris was proposed, although

radiology (including CT) showed no sign of prosthetic loosening. Metal ion chelating treatments were administered, which decreased metal ion concentrations, but caused only negligible neurological improvement. Resection arthroplasty was then carried out, during which infiltration of peri-prosthetic tissue by metallic debris was evident, and analysis of peri-prosthetic fluid showed high cobalt and chromium concentrations. Evident wear of the head and neck of the removed prosthesis supported the endogenous CoCr poisoning hypothesis. In the eight months following revision the patient showed progressive improvement, though vision was only partially improved. Metal ion concentrations improved, but remained higher than reference (57). This study recommends longer term follow up to evaluate adverse chronic systemic effects due to prolonged exposure to high serum cobalt concentrations (132), including neurological and toxicological examinations whenever a patient with a metallic prosthesis complains of visual loss and hearing disturbances, limb weakness, numbness or paraesthesia, even in the absence of osteoarticular symptoms.

1.4. Osteoblasts

Wear particles from artificial hip prostheses can induce many adverse cellular responses in the periprosthetic area, resulting in an inflammatory reaction and subsequent bone loss (50). Multiple cell types (macrophages, osteoclasts, osteoblasts, fibroblasts) are activated locally and secrete a range of pro-inflammatory cytokines and matrix metalloproteins (MMPs) (34-36, 133), e.g. IL-6 (134), IL-8 (81, 82), TNF- α (135), PGE₂ (80). These mediators contribute to an osteolytic cascade, resulting in the direct bone resorption by MMPs, or indirectly via osteoclast activation. Bone loss is a very serious risk with hip replacement, as it can lead to loosening, infection and reduce the overall lifespan of the device.

Bone is composed of different cell types and extracellular matrix (ECM), which becomes mineralized by calcium hydroxyapatite, which gives bone rigidity and

strength (136). Three distinct bone cells exist, two of which have interlinked functions; bone-forming osteoblasts and bone-resorbing osteoclasts (137). The balance between bone formation and resorption, known as bone remodelling, is paramount to healthy bone, and is carried out by factors secreted by osteoblasts, which regulate osteoclast differentiation, and factors secreted by osteocytes, the third distinct cell, which regulate the activity of both osteoblasts and osteoclasts (138). Therefore, the role of the osteoblast is very important in creation and maintenance of the skeletal architecture; as well as being responsible for bone formation, osteoblasts have the ability to regulate bone-resorption through the expression of these ligands, which link to pre-osteoclast receptors, inducing differentiation and causing bone resorption. Osteoblasts can also produce osteoprotegerin (OPG), which blocks this ligand action, preventing differentiation and resorption (139). Further coordination between osteoblasts and osteoclasts is mediated by the release of growth factors from bone during resorption (140).

The word osteoblast comes from the Greek words for 'bone' and 'germ'. They are cells of mesenchymal origin, and when terminally differentiated, they produce most of the ECM proteins, e.g. sialoprotein and osteocalcin, and control the mineralization of this matrix to form bone (137). Osteoblasts arise from osteoprogenitor cells located in deep periosteum layers and bone marrow, and are mono-nuclear, specialized cells, with a large golgi apparatus and an abundant rough endoplasmic reticulum when active. Osteoblasts form tight junctions with adjacent osteoblasts, and have regions of plasma membrane specialized in vesicular trafficking and secretion (141). The ability to secrete bone matrix arises as the osteoblasts differentiate (139).

1.4.1. Cobalt and Osteoblasts

Previous studies have shown that short-term exposure to metal species may affect human osteoclast and osteoblast function and survival (21); high concentrations of Co^{2+} (above 10 $\mu\text{g}/\text{mL}$) have been cytotoxic to osteoblasts and can reduce their cell

activity *in vitro* (142), including osteoblast proliferation (56, 142, 143), viability (56, 143) and function (142-144). Co^{2+} has proved more toxic than Cr^{3+} (50, 56). In the periprosthetic tissue, cobalt ions have induced local effects, such as apoptosis, necrosis, chemokine secretion (IL-8 and MCP-1) and TNF- α secretion in both macrophages and osteoblasts (50, 55, 56, 70, 84, 94, 95, 97, 98, 122). Cobalt and chromium have both inhibited the release of osteocalcin and the synthesis of Type I collagen from human osteogenic sarcoma cells (at concentrations of 10-100 ng/ml) (145). It has also been shown that short term exposure to cobalt ions at sub-lethal doses can decrease resorptive activity in rat osteoclasts (146). However, the longer-term effect of chronic exposure of human osteoblasts to clinically relevant cobalt ion concentrations is unknown. Queally *et al*, 2009, showed cobalt ions significantly reduce alkaline phosphatase activity and calcium deposition in human osteoblasts (50). This study was the first to demonstrate that cobalt ions stimulated the expression and secretion of chemokines from primary human osteoblasts, which contributes to osteolysis by the recruitment of inflammatory leukocytes and osteoclastic cells to the peri-prosthetic area and may interfere with bone ingrowth onto the implant (50). This study also showed that cobalt ions directly inhibited osteoblastic function, thereby possibly contributing to osteolysis by suppressing bone formation at the bone implant interface. The reduction in osteoblastic function has been directly correlated to the degree of toxicity, supporting the hypothesis that adverse local cellular responses (particularly necrotic responses) associated with metal debris from implanted metallic devices may be due in part to metal ions released from implants or from particulate debris (143). The importance of osteoblasts in overall bone regulation and function, and how this may be impeded by interaction with cobalt ions combined with the severity of osteolysis caused by MM hip prostheses forms the basis of why an osteoblast cell line was selected for cobalt toxicity testing in this project.

1.5. Calcium Channels

It is important to elucidate the mechanism by which cobalt ions enter cells and exert their effects, both locally and systemically, in order to gain a proper understanding of this toxicity and how it may be prevented in MM THA and HR patients. Cobalt is commonly regarded as a calcium channel blocker, with the ability to penetrate cells via calcium channels and reduce calcium influx (147-150). This gives rise to the hypothesis that cobalt may elicit its toxic effects via these channels. Also, previous literature has found that L-type calcium channels are present in osteoblasts (151), and the entry of cobalt through these channels may be the pathway by which cobalt wear particles induce osteolysis in patients with MM hip devices.

Calcium channels are ion channels in the plasma membrane permeable selectively to calcium ions and they can be ligand-gated or voltage-dependent (VDCC). VDCCs are found in all excitable cells (152, 153), including muscle, neurons, glial cells and, at lower levels in most non-excitable cells, such as osteoblasts (154). The development of Ca^{2+} signals is a tightly regulated cellular process involving concerted actions of plasma membrane and intracellular Ca^{2+} channels (154). VDCCs are closed at resting membrane potential and are activated (opened) in response to membrane depolarization, which allows Ca^{2+} enter the cell from extracellular space. The transient increase in intracellular calcium levels characterizes calcium signals and triggers a variety of physiological effects, depending on the cells involved, e.g. muscular contraction. Ca^{2+} channels, along with Na^{+} and K^{+} channels, form the superfamily of voltage-gated ion channels.

L-type calcium channels are a subset of VDCCs, and referring to the length of activation, the "L" stands for long-lasting. L-type calcium channels are widely expressed in skeletal muscle, smooth muscle and cardiac nodal tissue, where they are believed to play an important role in pacemaker currents and action potentials. However, the importance of L-type calcium channels in human physiology is not restricted to cardiovascular indications; they have been found in neurons, and bone,

endocrine and sensory cells, and play roles in neuronal plasticity (155), modulation of neuronal firing (156) and gene-expression (157), memory (158), controlling mood and drug-related behaviours (159, 160), vision and hearing (161), the release of a variety of hormones and neurotransmitter, and skeletal muscle contraction (162).

1.5.1. Calcium Channels and Osteoblasts

Duncan *et al*, 1998, reported that calcium channels play fundamental roles in cellular responses to external stimuli, including mechanical forces and hormonal signals in osteoblasts and bone cells of osteoblast lineage (154). Previous literature (163, 164) reports L-type VDCCs playing an important role in the influx of Ca^{2+} into osteoblasts after a mechanical stimulus. Calcium channel blocker nifedipine has shown the ability to reverse a mechanically-induced increase in extracellular matrix proteins, osteopontin and osteocalcin (163), and another previous study has shown that *in vivo* blockage of L-type VDCCs by both nifedipine and verapamil, another calcium channel blocker, substantially suppressed a mechanically-induced bone formation increase (165). Inhibition of L-type VDCCs, removal of extracellular Ca^{2+} and plasma membrane depolarization could inhibit gap junction-mediated intracellular calcium signalling in osteoblast cells (166).

Another study found that parathyroid hormone (PTH) and mechanical loading might act synergistically on bone formation *in vivo* (167). Mechanical loading and PTH together enhanced bone formation significantly, and this enhancement was found to be suppressed by verapamil, indicating that L-type VDCCs mediate load-induced bone formation and enhancement of bone adaptation by PTH *in vivo*. Previous literature also describes how verapamil and nifedipine interact with osteoblasts via L-type VDCCs, promoting their differentiation by stimulating alkaline phosphatase activity (168). Regulation of bone turnover is complex and regulated by many factors, including hormones, growth factors, cytokines, etc. (169), but little is known about the signals coupling bone formation to bone resorption. L-type calcium channels are also proposed to modulate paracrine signals between bone-forming

osteoblasts and bone-resorbing osteoclasts at local sites of bone remodelling (154, 170), and signalling between these bone cells is important in bone homeostasis and regulating bone remodelling (169, 171, 172).

1.5.2. Calcium Channel Blockers

A calcium channel blocker (CCB) is a chemical that disrupts the movement of calcium (Ca^{2+}) through calcium channels and they have widespread clinical uses as anti-arrhythmics and anti-hypertensives. Currently approved CCBs bind to L-type calcium channels and by blocking calcium entry into vascular and cardiac cells, they exert vasodilative and cardiodepressive properties, e.g. decreased contractility, heart rate and conduction velocity. Vasodilation causes a reduction in total peripheral resistance, while decreased contractility reduces cardiac output, and the end result is a drop in blood pressure. CCBs are also used in the treatment of angina pectoris pain, which is caused by a deficient oxygen supply to the heart – vasodilation increases cardiac blood and oxygen supply.

There are three classes of CCBs that bind specifically to L-type VDCCs (165), which differ in chemical structure as well as their selectivity for cardiac or vascular L-type VDCCs. Dihydropyridines, e.g. nifedipine, have high vascular selectivity; phenylalkamines, e.g. verapamil, are relatively selective for the myocardium and less effective as vasodilators; and benzothiazepines, e.g. diltiazem, have both cardiodepressive and vasodilative actions.

1.5.2.1. Verapamil and Nifedipine

90-100% of verapamil is absorbed when administered orally, but due to a high first-pass metabolism, bioavailability is in the much lower 20-35% range. It is 90% bound to plasma proteins and has a volume of distribution of 3-5 L/kg. It is metabolised in the liver to ~12 inactive metabolites, 70% of which are excreted as metabolites by the kidneys. Onset of action is 1-2 hours after oral dosage and the half-life with

chronic doses is 4.5-12 hours (173). Verapamil is used in the treatment of angina, arrhythmias and hypertension.

Nifedipine has a bioavailability of 84-89%, when administered in extended release form, with 92-98% binding to protein. It has a half life of ~2 hours; 7 hours for extended release nifedipine. It is metabolised by gastrointestinal and hepatic means and 60-80% is excreted renally as metabolites. Patients are warned against consuming grapefruit or grapefruit juice while taking nifedipine, as the drug interaction raises the blood level of nifedipine, possibly by lowering CYP3A4 activity (174). Nifedipine is used in the treatment of hypertension.

1.6. Aim of Project

Previous studies on primary human osteoblasts showed effects at nifedipine concentrations of 10 μM , where it significantly altered TGF- β 1 calcium signalling increases in α 5 integrin expression (172). Similarly, human osteoblast-like cells, SaSO-2, treated with 10 μM verapamil for 30 minutes significantly inhibited a shear-stress induced increase in TGF- β 1 mRNA levels, with which L-type voltage-gated calcium channels are believed to be involved (175). Verapamil was seen to elicit therapeutic effects at lower doses also; one experiment utilising an osteoblast-like clonal osteosarcoma cell line found that treating cells for 90 days with 1.5 μM verapamil was sufficient to inhibit a PTH-induced increase in free cytosolic calcium by 50% (176), by blockade of phase I calcium channels. Based on these observations, a range of 0.1 – 100 μM was used, with the belief that the therapeutic concentration desired would fall between these two concentrations.

Cobalt was used in the concentration range 0.1 – 200 μM in accordance with previous literature; Using SaOS-2 cells, Zijlstra *et al*, 2012, carried out their experiment with concentrations of 1, 10 and 100 μM , reporting significant reductions in the number of osteoblast like cells, compared to control groups, at 10 and 100 μM , after 24, 48, 72 and 96 hours (177). This range of cobalt concentrations

correlates with elevated circulating cobalt levels recorded in previous literature in whole blood, up to 4.6 μM (65), and local hip synovial fluid, up to 30 μM (66) following MM THA. Also, *in vivo* cobalt levels in Australian journal Mao *et al*, 2011, were recorded in serum at 185 – 410 nmol/L (0.185 – 0.410 μM) and joint fluid at 4218 nmol/L (4.218 μM), and these also fell within the concentration parameters of this project (58).

Although L-type VDCC blockers have previously been claimed to elicit inhibitory effects on osteoblastic function, and their long-term use can produce adverse effects on normal bone metabolism, the aim of this experiment is to find the maximum dose of verapamil and nifedipine tolerated by the OST 5 cells *in vitro*, in a bid to elicit therapeutic effects without causing toxicity. Investigation will then be carried out into whether, at this therapeutic dose, the CCBs will prevent the cobalt-induced toxicity in the OST 5 cells. If it were possible to elucidate beyond doubt that cobalt elicits its toxicity via L-type voltage-gated calcium channels, and if it were possible to control these effects by blockade of these channels, it could help eradicate metal toxicity in MMTHA patients, reducing pain, distress and other symptoms, and ultimately the need for revision.

To summarize, the aim of this project is:

- Measure the acute effects of exposure to increasing concentrations of cobalt ions on OST 5 cell *in vitro* to discover the concentrations at which toxicity occurs
- Measure the acute effects of exposure to increasing concentrations of calcium channel blockers, nifedipine and verapamil, on OST 5 cells to discover the highest concentrations at which toxicity does not occur
- Elucidate whether cobalt ions act via calcium channels by investigating whether cells pre-treated with a toxic concentration of cobalt would show reduced toxicity when a non-toxic concentration of calcium channel blocker is also administered; i.e. discover whether calcium channel blockers can prevent cobalt-induced toxicity in OST 5 cells *in vitro*.

2. Materials and Methods

Table 2.1: A List of all chemicals used throughout the course of the experiment, and the laboratory from which they originated. Chemicals were Analar grade where appropriate.

Material	Laboratory
Sabouraud Dextrose Liquid Medium	Oxoid, UK
Brain Heart Infusion Broth	Oxoid, UK
Versene	Sigma Aldrich, UK
Trypsin	Sigma Aldrich, UK
Dulbecco's Modified Eagle Medium (DMEM)	Lonza, UK
Penicillin/Streptomycin	Sigma Aldrich, UK
Non-Essential Amino Acids (NEAA)	Lonza, UK
Foetal Bovine Serum (FBS)	Biosera, UK
Cobalt Chloride	Alfa Aesar, UK
Nifedipine	Sigma Aldrich, UK
Verapamil	Sigma Aldrich, UK
DMSO	Sigma Aldrich, UK
PBS	Sigma Aldrich, UK
NR	Sigma Aldrich, UK
MTT	Sigma Aldrich, UK
Ethanol	Sigma Aldrich, UK
Glacial Acetic Acid	BDH, UK
Phalloidin-FITC	Sigma Aldrich, UK
Methanol	Fisher, UK
Bovine Serum Albumin (BSA)	Sigma Aldrich, UK
Formalin	Sigma Aldrich, UK

Immunomount Mounting Fluid	Thermo Electron, USA
Propidium Iodide	Invitrogen, UK
CFDA	Invitrogen, UK

2.1. OST 5 Cells

Ost 5 cells are a rat osteoblast cell line cultured *in vitro* with a ~10% foetal bovine serum medium, non-essential amino acids and penicillin/streptomycin in an incubator at 37°C. Prior to beginning experimentation, it was ensured that the OST 5 cells tested negative for bacteria and fungi by incubation with microorganism culture media, Sabouraud Dextrose Liquid Medium and Brain Heart Infusion Broth, and were therefore considered sterile. All work on OST 5 cells, up to the point of preparation for cell viability assays, was carried out in a class II Laminar flow hood, which provided the aseptic environment necessary for cell culture experiments.

2.1.1. Medium Preparation

Dulbecco's Modified Eagle Medium (DMEM) was used, which is a cell culture medium containing a higher concentration of amino acids, vitamins and glucose than many other media types. To 500 mL DMEM, 50 mL Bovine Foetal Serum (BFS) was added to supply the cells with growth factors. 5 mL each of streptomycin/penicillin and non-essential amino acids were also added as an antibiotic to prevent bacterial infection occurring in the cell culture and to reduce the metabolic burden on the cells and allow cell proliferation, respectively. Medium is kept at 4 °C and must be pre-warmed to 37 °C before using.

2.1.2. Passaging Cells

Cells were passaged twice a week, to prevent the cultures becoming over confluent. On Thursdays, a small (5 mL) culture flask was passaged, in a split ratio of 1:10 to

reduce cell numbers, into a large (75 cm²) and a fresh small (25 cm²) flask. On Mondays, the small flask was passaged as before into another small flask, and the contents of the large flask were used experimentally. All surplus material was discarded. The flask was emptied of medium and washed out twice with versene (large flask – 10 mL; small flask – 5 mL), before 1-2 mL trypsin-versene was added and the flask was allowed to stand for ~5 minutes. **Versene/EDTA (ethylenediaminetetraacetic acid)** is a chelating agent which lifts certain cells into suspension by binding to metal cations. Combined **trypsin-versene** removes cells from the bottom of the flask into suspension, by cleaving proteins which bond the cells to the flask. Versene was added to trypsin to enhance its activity, by removing extracellular matrix calcium and magnesium, exposing the peptide bonds of the cell surfaces to hydrolysis by trypsin. Versene was stored at room temperature, and trypsin-versene was stored frozen at 0 °C, and was placed in a 37 °C incubator to thaw before using. After passaging, culture solutions were made up to 10 mL and 30 mL in small and large flasks respectively with medium.

2.1.3. Counting Cells

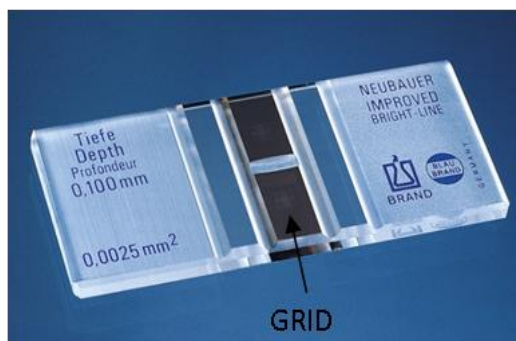


Figure 2.1: Haemocytometer

On Monday (day 1) of experimental weeks, medium was emptied from the large flask and the cell culture was washed twice with versene and 2 mL of trypsin-versene is added to lift cells into suspension. The flask often needed to be tapped to ensure all cells became detached. The content of the flask was

made up to 10 mL with medium, and when homogenous, a pipette was used to apply 0.1 mL of cell solution to a haemocytometer slide, covered with a cover slip, for cell counting. The OST 5 cells were then viewed on the 3x3 haemocytometer grid under a microscope, and were counted in the top left and bottom right box

using a cell counter (including cells resting on the top and left lines of each box) and the average (A) of these two figures was obtained – $A \times 10^4$ = the number of cells/mL of solution.

96 well plates were used, and approximately 5×10^3 cells were placed in each well, a number that was subsequently reduced to 2.5×10^3 cells after cells were visibly over-confluent in week 1. Depending on how many plates were needed per week, the desired cell number was multiplied by the number of wells to be used. The total cell number needed was then divided by the cells/mL reading calculated by the haemocytometer cell counting to give the volume of cell solution needed.

$$\frac{\text{Total number of cells needed for all wells}}{\text{Calculated cells/mL}} = \text{Volume of cell solution needed (mL)}$$

The total medium volume to fill each well with 200 μ L of media, whilst ensuring that approximately the correct cell number was placed in each well, was calculated by the following equation:

$$\text{Total number of wells used} \times \text{volume per well (200 } \mu\text{L)} = \text{Total medium volume}$$

The total medium volume consisted of the calculated volume of cell solution needed from the above equation, made up to the correct volume with medium. When the solution had been correctly prepared, a multiple-tipped pipette and troughs were used to place 200 μ L of the solution into all wells of each plate being used, with the exception of outer wells, which are prone to more evaporation in the incubator, and therefore cells were not placed here. Pipette tips and troughs were sterilised by microwaving for 5 minutes before use. Well plates were then incubated for 24 hours to ensure the cells were firmly attached to the bottom of wells before

medium was removed and concentrations of cobalt or calcium channel blockers were applied to the cells.

2.2. Cobalt Concentrations

Solid cobalt chloride ($\text{CoCl}_2 \cdot 6\text{H}_2\text{O}$) (MW = 237.93) was diluted in distilled H_2O to make a 10 mM stock solution (0.0594825 g/25 mL), which was passed through a 0.2 μM filter to remove any contaminants and stored at 4°C. The stock solution was then diluted with medium to obtain various concentrations in the range of 1 – 200 μM over the course of the 6 week experimentation period.

2.3. Nifedipine Concentrations

Solid nifedipine (MW = 346.3) is insoluble in H_2O , and was therefore diluted in DMSO to make a 100 mM stock solution (0.3463 g/10 mL). The stock solution must be 100 mM, as opposed to 10 mM, as the vehicle DMSO is toxic to cells in high concentrations and must be diluted 1000-fold (i.e. 0.1% DMSO). This stock solution need not be filtered as DMSO will not support any bacterial growth, and can be stored at 4 °C. The nifedipine stock solution was then diluted serially using medium to make concentrations in the range of 0.1 – 100 μM and was used as a calcium channel blocker in week 3.

2.4. Verapamil Concentrations

Solid verapamil (MW = 491.9) was diluted in distilled H_2O to make a 10 mM stock solution (0.123 g/25 mL) and passed through a 0.2 μM filter to remove impurities. Again, this solution was stored at 4 °C. Dilutions were carried out on the stock solution with medium to make concentrations in the same concentration range as

with nifedipine (0.1 – 100 μM) and was used as a calcium channel blocker in weeks 4 through to 6.

2.5. Administration of Cobalt, Nifedipine and Verapamil to OST 5 Cells

Weeks 1 and 2

Varying concentrations of cobalt were added to the OST 5 cells 24 hours after seeding the cells in well plates, with the aim of assessing the effect of the metal on cell viability and growth. In week 1, concentrations of 1 – 100 μM of cobalt were used and viability was quantified by NR and MTT assays at 24 and 48 hours. In week 2, concentrations of 10 – 200 μM were used, and viability was quantified at 72 hours, in addition to at 24 and 48 hours, post cobalt treatment. The control in these weeks was medium.

Table 2.1: Dilution procedure for final cobalt concentrations in week 1

Concentration	Volume of Cobalt Stock (10 mM)	Volume of Medium	Rows of Wellplate	Final Volume	Dilution Factor (from stock)
100 μM (A)	200 μL	19.8 mL	10, 11	20 mL	1:100
50 μM (B)	100 μL	19.9 mL	8, 9	20 mL	1:200
10 μM (C)	20 μL	19.98 mL	6, 7	20 mL	1:1000
1 μM (D)	2 mL (Sol. C)	18 mL	4, 5	20 mL	1:10 (from 10 μM)
Control	-	20 mL	2, 3	20 mL	-

Weeks 3 and 4

Nifedipine and verapamil were added in increasing concentrations to the OST 5 cells 24 hours after cell seeding in weeks 3 and 4, respectively, to assess the LD₅₀ of these calcium channel blockers, in a bid to identify the drug which causes the least toxic effects to the OST 5 cells. The less toxic of these drugs would then be used as a calcium channel blocker in an attempt to block cobalt entry into cells and counteract the cobalt-induced toxicity. NR and MTT assays were again used to assess toxicity of both drugs. The control in these assays was medium, but in the case of nifedipine, 0.1% DMSO was necessary in the control medium, as a vehicle control, to avoid inaccuracies in assessing toxicity.

Table 2.2: Dilution procedure for final nifedipine concentrations in week 3

Concentration	Volume of Nifedipine (100 mM)	Volume of Medium	Rows of Wellplate	Final Volume	Dilution Factor
100 µM (A)	25 µL	24.975 mL	10, 11	25 mL	1:1000
10 µM (B)	2.5 mL (Sol A)	22.5 mL	8, 9	25 mL	1:10 (from Sol A)
1 µM (C)	2.5 mL (Sol B)	22.5 mL	6, 7	25 mL	1:10 (from Sol B)
0.1 µM (D)	2.5 mL (Sol D)	22.5 mL	4, 5	25 mL	1:10 (from Sol C)
Control	-	24.975 mL (25 µL DMSO – 0.1%)	2, 3	25 mL	-

Table 2.3: Dilution procedure for final verapamil concentrations in week 4

Concentration	Volume of Verapamil (10 mM)	Volume of Medium	Rows of Wellplate	Final Volume	Dilution Factor
100 μ M (A)	250 μ L	24.75 mL	10, 11	25 mL	1:100
10 μ M (B)	2.5 mL (Sol A)	22.5 mL	8, 9	25 mL	1:10 (from Sol A)
1 μ M (C)	2.5 mL (Sol B)	22.5 mL	6, 7	25 mL	1:10 (from Sol B)
0.1 μ M (D)	2.5 mL (Sol C)	22.5 mL	4, 5	25 mL	1:10 (from Sol C)
Control	-	25 mL	2, 3	25 mL	-

Also in weeks 3 and 4, the respective drug was added to separate plates of OST 5 cells at 24 hours after cell seeding for 2 hours in a bid to block calcium channels before any administration of cobalt, after which the drug was removed and a combination of calcium channel blocker (increasing concentrations) and cobalt (fixed concentration) was added to the wells. 100 μ M was the cobalt concentration chosen, as this had shown to be toxic in weeks 1 and 2. The control in these assays was 100 μ M cobalt, and this served to assess if the addition of calcium channel blocker will result in toxicity being lower in these wells, than in cobalt-only wells.

All plates at weeks 3 and 4 underwent MTT and NR assays at 24 and 48 hours.

Table 2.4: Dilution procedure for combined cobalt and nifedipine concentrations in week 3

Nifedipine Concentration	Cobalt Concentration	Volume of Nifedipine (100 mM)	Volume of Cobalt (10 mM)	Volume of Medium	Final Volume
100 μ M	100 μ M	10 μ L	100 μ L	9.89 mL	10 mL
10 μ M	100 μ M	1 mL Sol A (Table 2.2)	100 μ L	8.9 mL	10 mL
1 μ M	100 μ M	1 mL Sol B (Table 2.2)	100 μ L	8.9 mL	10 mL
0.1 μ M	100 μ M	1 mL Sol C (Table 2.2)	100 μ L	8.9 mL	10 mL
Control	100 μ M	-	100 μ L	9.9 mL	10 mL

Table 2.5: Dilution procedure for combined cobalt and verapamil concentrations in week 4

Verapamil Concentration	Cobalt Concentration	Volume of Verapamil (10 mM)	Volume of Cobalt (10 mM)	Volume of Medium	Final Volume
100 μ M	100 μ M	100 μ L	100 μ L	9.80 mL	10 mL
10 μ M	100 μ M	1 mL Sol A (Table 2.3)	100 μ L	8.9 mL	10 mL
1 μ M	100 μ M	1 mL Sol B (Table 2.3)	100 μ L	8.9 mL	10 mL
0.1 μ M	100 μ M	1 mL Sol C (Table 2.3)	100 μ L	8.9 mL	10 mL
Control	100 μ M	-	100 μ L	9.9 mL	10 mL

Weeks 5 and 6

In weeks 5 and 6, four 24 hour cell-seeded plates were treated with increasing concentrations of cobalt (MTT and NR at 24 and 48 hours), for which the control was medium.

A further 4 plates were treated with 10 μ M verapamil for 2 hours, which was then removed and a combination of cobalt (increasing concentrations) and verapamil (fixed concentration) was added. Verapamil was chosen as the calcium channel blocker in the final weeks of experimentation, as it exhibited a much lower LD₅₀ than nifedipine, and a 10 μ M concentration was chosen as no toxic effects were apparent at this level in week 3. The aim in weeks 3 and 4 was to compare the viability of cobalt treated cells with cobalt and verapamil treated cells, to attempt to quantify the ability of verapamil to reduce the toxic effects of cobalt on OST 5 cells, and thus help to elucidate whether cobalt-induced toxicity takes place via calcium channels.

Table 2.6: Dilution procedure for combined cobalt (alternations) and verapamil (fixed) concentrations in weeks 5 and 6

Verapamil Concentration	Cobalt Concentration	Volume of Verapamil (10 mM)	Volume of Cobalt (10 mM)	Volume of Medium	Final Volume
10 μ M	200 μ M	15 μ L	300 μ L	14.685 mL	15 mL
10 μ M	100 μ M	15 μ L	150 μ L	14.835 mL	15 mL
10 μ M	50 μ M	15 μ L	75 μ L	14.910 mL	15 mL
10 μ M	10 μ M	15 μ L	15 μ L	14.970 mL	15 mL
10 μ M	Control	15 μ L	-	14.985 mL	15 mL

2.6. Viability Assays

The spectrophotometer used for all cell viability assays was a Shimadzu UV-Vis UV-2401PC, and the plate reader used was a Labsystems Multiskan Ascent.

2.6.1. PBS

Two phosphate buffer solutions (PBS) were made up by dissolving PBS tablets in 500 ml distilled water. Naturally assuming a pH of 7.4, one PBS solution was left at this pH, while HCL was added dropwise to the other solution to get a pH of 6.75.

2.6.2. Neutral Red

Neutral red (NR) is used as a vital stain. It readily penetrates the cell membranes of viable cells and, being slightly cationic, binds to anionic sites on the lysosomal matrix. As neutral red accumulates in the lysosomes, the colour intensity increases (178).

5 mg neutral red is dissolved in 100 ml neutral pH PBS, incubated overnight at 37 °C and passed through a 0.2 µm filter, to remove any undissolved crystals remaining. This can be stored at 4 °C for several weeks.

Method

When cells are ready for NR staining, all surrounding medium was removed, 100 µL NR solution was added to each well and the plate was incubated at 37 °C for 3 hours. NR was then removed, and each well washed with 200 µL neutral PBS. 100 µL destain was then added to each well, and the plate was shaken for ~30 minutes, or until a homogenous colour was seen in all wells, allowing a better determination of viability, expressed as colour intensity. Destain was created by adding 1 mL glacial acetic acid to 50 mL ethanol and 49 mL distilled H₂O in a fume hood.

Absorbance was measured at 540 nm, after the plate reader has been allowed warm up for ~30 minutes.

2.6.3. MTT

MTT assays are colorimetric viability assays which measure enzyme activity in living cells, by the ability of the enzymes to reduce MTT to formazan, which gives a purple colour. Dimethyl sulfoxide (DMSO) is used to dissolve the purple formazan produced into a soluble, coloured solution, the absorbance of which can be quantified by a spectrometer.

A 10 mM MTT solution was made up by dissolving 0.4143 g MTT in 100 ml PBS pH 6.75, and filtering the resulting solution through a 0.2 μm filter to remove undissolved crystals. At 4 °C, the MTT solution can be stored for 2 weeks.

Method

Once cells are ready, the surrounding medium was removed from all wells, before the addition of 50 μL of MTT solution to each well and the plate was incubated for 4 hours at 37 °C. The MTT solution was then removed by pipette, removing as much as possible so as not to affect the final colour, whilst taking care not to remove the formazan product created. Plates were centrifuged (5 minutes at ~3500 rpm) to ensure cells remain at the bottom of the wells. 200 μL DMSO was added to dissolve formazan, and was mixed to an even colour by pipetting up and down twice in each well before the absorbance is read at 540 nm.

2.7. Confocal Microscopy and Photography

In week 7, OST 5 cells were set up and stained with a number of chemicals to be viewed under a confocal microscope and photographed. Cells were seeded in either

24 well plates, 1.56×10^4 cells per 2 cm^2 well, or 9.6 cm^2 petri dishes, 7.5×10^4 cells per dish. After 24 hours, seeded cells were divided into four groups, with 2 dishes/wells per group: medium only control; cobalt only sample (100 μM); verapamil only sample (10 μM); combined cobalt and verapamil sample (100 and 10 μM respectively). Staining, viewing and photography all took place at 48 hours post treatment, where, based on assay results, effects were more likely to be seen than at 24 hours. The confocal microscope used for the following was a Carl Zeiss Axio Imager Microscope and the software used alongside the microscope was Axiovision 4.6.

2.7.1. Staining for Actin using Phalloidin-FITC

Phalloidin binds in a highly-selective manner to actin, a protein found in all eukaryotic cells, which forms microfilaments, and is a cytoskeletal subclass. The main function of actin is to mechanically support cells and provide routes for cytoplasmic trafficking and signal transduction (179). Phalloidin can be labelled with fluorescent analogues to investigate in high-contrast the distribution of the protein using light microscopy, in this case, the fluorescent green dye fluorescein (FITC). In this experiment, phalloidin-FITC was used to determine the structure of the cytoskeleton in each case, and observe the effects that verapamil and cobalt had on OST 5 cells in comparison with the control sample, and the combined cobalt and verapamil treated sample.

Phalloidin is an extremely toxic substance, a peptide isolated from the *Amanita phalloides* 'death cap' mushroom. It must be handled with care and all waste must be disposed of through correct chemical means; collected in appropriate, labelled containers taking care to ensure no phalloidin or washings enter drains, and disposal is entrusted to an Industrial Waste Disposal Company.

0.1 mg Phalloidin-FITC was dissolved in 1 mL methanol, injected directly into the vial through the rubber seal without opening it. This is carried out in a fume hood for safety. 4 mL 1% w/v BSA (bovine serum albumin) in PBS was added, giving a dilution

of 1/50. The solution was aliquoted into Eppendorff tubes and stored at -20 °C in the dark.

Method

OST 5 cells are seeded in 24 well plates on 13 mm diameter glass coverslips. After the designated time, medium is removed and the wells are washed with warm PBS (37 °C). The cells are then fixed with 4% formalin in PBS in the fume hood for 20 minutes, before being washed three times with PBS.

Staining

During the staining preparations, all materials must be kept in the dark (i.e. under tin foil, or a dark container). The cells were incubated with Phalloidin-FITC (diluted to 1/500 in PBS – a 1/10 dilution in PBS was performed on the 1/50 Phalloidin-FITC above) in a moist chamber for 1 hour, before being washed three times in PBS (the cells being allowed to steep in PBS for 5 minutes each time). Glass coverslips were removed from wells using forceps, excess PBS drops were removed and they were affixed to slides using Immunomount mounting fluid and viewed using fluorescence microscopy with a dry lens at magnification of x20.

2.7.2. Cell Viability Staining using Propidium Iodide and CFDA

Propidium Iodide (PI) is a fluorescent, intercalating agent used as a DNA stain in cell viability evaluation. It can be used to differentiate between apoptotic, necrotic and normal cells. It binds to DNA, intercalating between bases and once bound, it fluoresces. Cell permeable dye, carboxyfluorescein diacetate (CFDA) gives a strong, detectable green fluorescence, produced by hydrolysis inside the cell, with negligible cell death. PI produces red fluorescence by interacting with the nuclei of dead cells. Cell Viability can be detected by observing the ratio of green stain

(representing live cells) to red stain (representing dead cells) visible under the microscope.

200 µg Propidium Iodide (PI) was diluted in 20 mL PBS pH 7.4. As CFDA may leak from cells with time, cells must be prepared for staining and viewed one at a time, to avoid specimens standing for prolonged periods of time, which may impair viewing.

Method

The medium was removed from all petri dishes, which were then washed twice with neutral PBS. 2 mL PI was added to petri dishes and they were incubated in the dark for 1 minute. PI was removed and discarded to the appropriate waste bottle, and dishes were washed a further three times with neutral PBS, the washes being discarded to the same waste bottle. 2 mL CFDA (25 µM in pH 6.75 PBS – CFDA is pH dependent, and must be used with PBS at pH 6.75) was added to dishes and they were incubated in the dark at room temperature for 5 minutes. CFDA was removed and discarded in a separate waste bottle, and cells were washed three times with pH 6.75 PBS, which was discarded to the same waste bottle as the CFDA. 3ml pH 6.75 PBS was added to each petri dish, and specimens were viewed immediately using fluorescence microscopy at 620 nm with a wet lens at a magnification of x20.

2.8. Statistics

Statistics were performed using Minitab software, version 16. One way Analysis of Variance (ANOVA) testing was performed to compare absorbance means of different concentration groups and controls in cobalt, nifedipine and verapamil-treated cells. When significance was seen between means of test groups, Post Hoc Fisher LSD (least significant difference) testing was carried out to explore all possible pair-wise comparisons for significance.

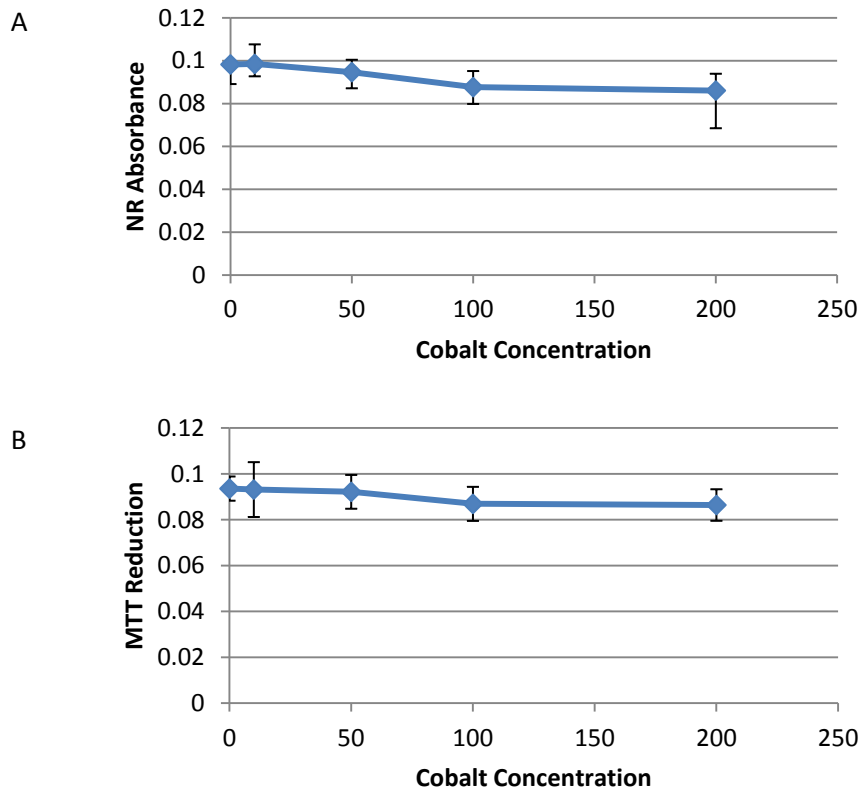
Independent 2-sample Student's t-tests compared cobalt-treated cells with cobalt and verapamil-treated cells at each concentration of cobalt. This test is used as the samples, from two different populations, are independent of each other, with a similar distribution. Microsoft Excel was used to plot scatter graphs of viability results and dose-response curves of cobalt and calcium channel blockers, from which the LD₅₀ values could be obtained.

3. Results

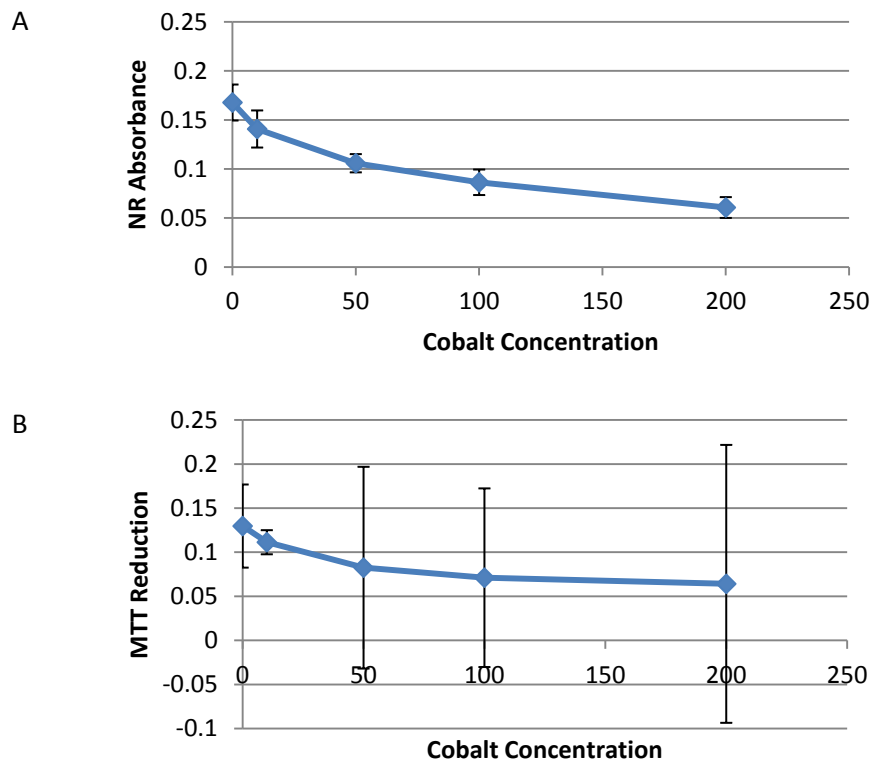
3.1. Effect of Cobalt on OST 5 Cell Viability

Data on graphs are expressed as the concentration of cobalt versus the value of NR absorbance or the reduction of MTT, which are both directly proportional to cell viability, as these actions are a measure of live cellular activity. A decrease in NR absorption and MTT reduction is indicative of a decrease in cell viability.

Cobalt-treated OST 5 cells showed a dose-dependent decrease in NR absorbance and MTT reduction. This was apparent at 24 hours post cobalt treatment, but a greater effect was seen after 48 hours (see graph 3.2). At 24 hours, both NR (A) and MTT (B) assays showed similar absorbance/reduction scores. At 48 hours, there was more variation between the two assays, with NR (A) showing slightly higher scores at lower concentrations than MTT (B), but both expressed similar absorbance/reduction scores at the highest concentration used (200 μ M). In week 2, viability was also assessed at 72 hours post cobalt-treatment, but as similar results to those of 48 hour post treatment were yielded here, this time point was not used again. Also, it was decided that a concentration of 100 μ M cobalt would be used in subsequent experimental stages, where a fixed control of cobalt was needed, as toxicity was evident at this concentration.



Graph 3.1: The effect of increasing concentrations of cobalt on the viability of OST 5 cells at 24 hours, shown by NR (A) and MTT (B) assays. Cobalt was seen to decrease cell viability in a dose-dependent manner. Data are expressed as mean±SD; n = 12. ANOVA testing showed significant differences between control and cobalt-treated groups in NR and MTT assays. $p > 0.05$. Post-hoc Fisher analysis found significant differences at 24 hours in comparing the control group with 100 and 200 μM; 10 μM with 100 (just NR) and 200 μM; 50 μM with 200 μM (just NR); CI = 95%.

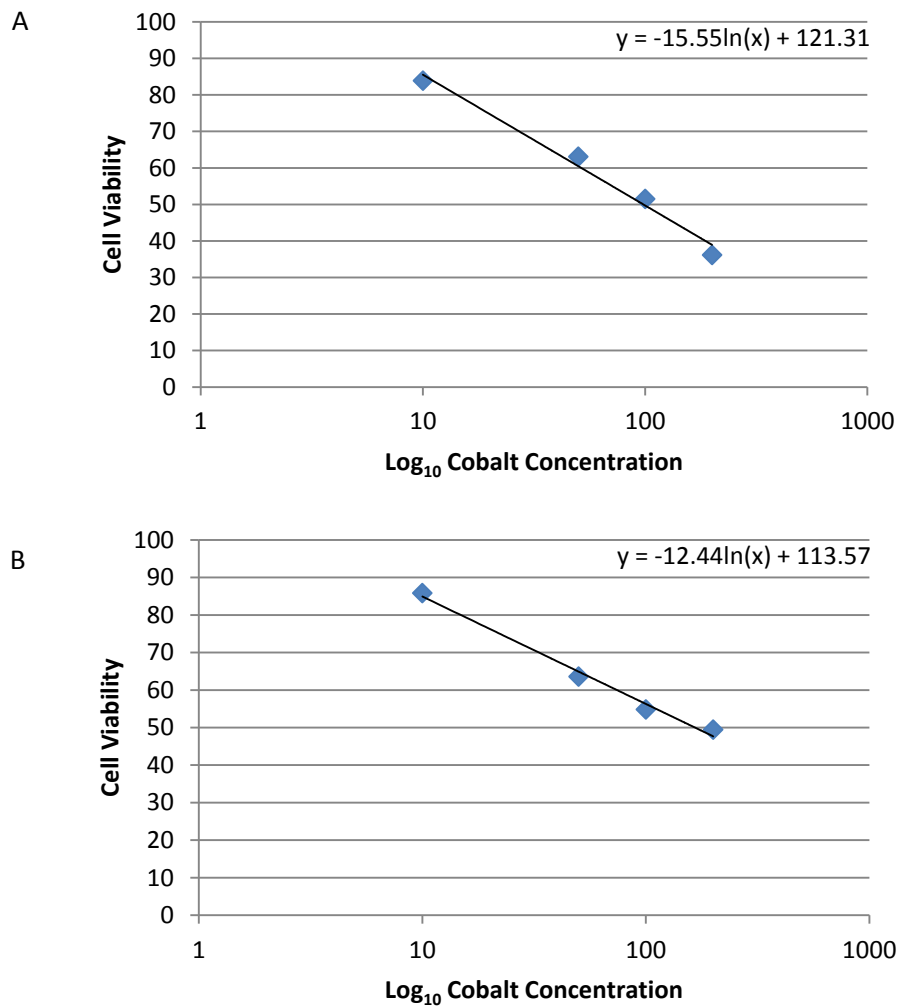


Graph 3.2: The effect of increasing concentrations of cobalt on the viability of OST 5 cells at 48 hours, shown by NR (A) and MTT (B) assays. Cobalt was seen to decrease cell viability in a dose-dependent manner. Data are expressed as mean±SD; n = 12. ANOVA testing showed significant differences between control and cobalt-treated groups in NR assay, but failed to identify significant differences in MTT assays at 48 hours; $p > 0.05$. Post-hoc Fisher analysis found significant differences at 48 hours between all groups in NR assay, but no significance was seen between any groups in MTT assay: CI = 95%.

The absorbance data were statistically analysed using Minitab 16, and attempts were made to significantly distinguish the means of control groups from cobalt-treated groups using one-way Analysis of Variance (ANOVA). The null hypothesis, being that the mean of all groups was equal, was rejected in the NR and MTT assays at 24 and the NR assay at 48 hours, indicating significant differences between cobalt-treated cells and the control-untreated cells in these assays. Significance was not seen in the 48 hour MTT assay. However, ANOVA testing does not provide sufficient information on the individual groups, and Post-hoc Fisher analysis was therefore performed to elucidate which cobalt-treated cell groups differed

significantly from the control and from each other. Significant differences between various groups were seen in both MTT and NR assays, with the exception of the MTT assay at 48 hours. In the 24 hour NR and MTT assays, significant differences were seen when comparing the control group to the 100 and 200 μM groups, comparing 10 μM with 200 μM group, and in the NR, but not the MTT assay, significant difference was seen between the 10 and 100 μM groups and the 50 and 200 μM treated cells. At 48 hours, Post-hoc Fisher analysis showed significant differences between all groups of the NR assay.

Dose response curves were constructed from the MTT and NR assay results, expressing all results as a percentage of the control and plotting against the \log_{10} concentration of cobalt to obtain LD_{50} values. At 48 hours post cobalt treatment, the LD_{50} values were calculated as 98.08 μM from the NR assay and 169.69 μM from the MTT assay. This offered further suggestion that a concentration of 100 μM cobalt is a sufficiently toxic level of the metal to allow us to subsequently investigate the effect of calcium channel blockers on the toxicity.



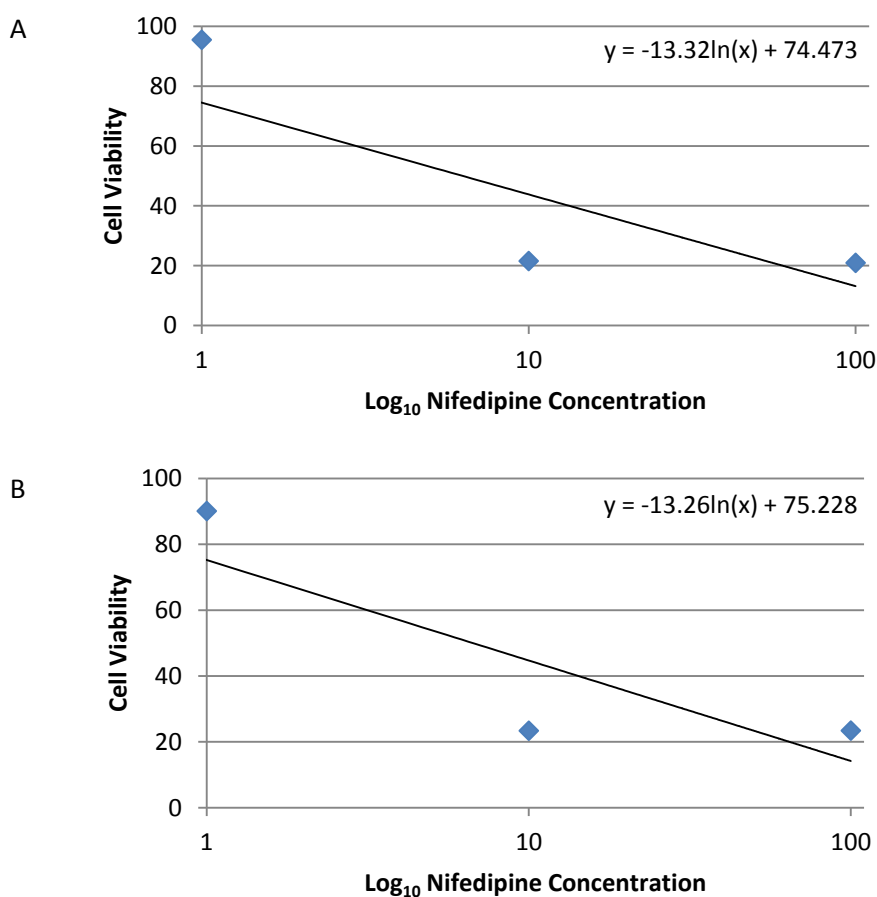
Graph 3.3: Dose response curves were plotted, viability versus the log₁₀ scale of cobalt concentration, to obtain LD₅₀ values shown by NR (A) – 98.08 μM; and MTT (B) – 169.69 μM at 48 hours; n = 12.

3.2. Effect of Nifedipine on OST 5 Cell Viability

3.2.1. Nifedipine

Nifedipine was the first of two calcium channel blockers to be used experimentally in a bid to prevent cobalt-induced toxicity in these cells by blocking entry of the

metal ions, and dose-response curves were again plotted to obtain the LD₅₀ of nifedipine. Ideally, the calcium channel blocker would have as high an LD₅₀ as possible while still exerting its desired effect; it would block the calcium channels effectively, while producing a low toxic response in the cells. However, the LD₅₀ values obtained at 48 hours post nifedipine treatment from the NR and MTT assays, although consistent with each other, were considerably lower than those for cobalt, at 6.28 and 6.70 μM, respectively. According to these results, nifedipine is a more toxic chemical than cobalt to OST 5 cells, an undesirable trait for a calcium channel blocker in this experiment (refer to *graph 3.4*).



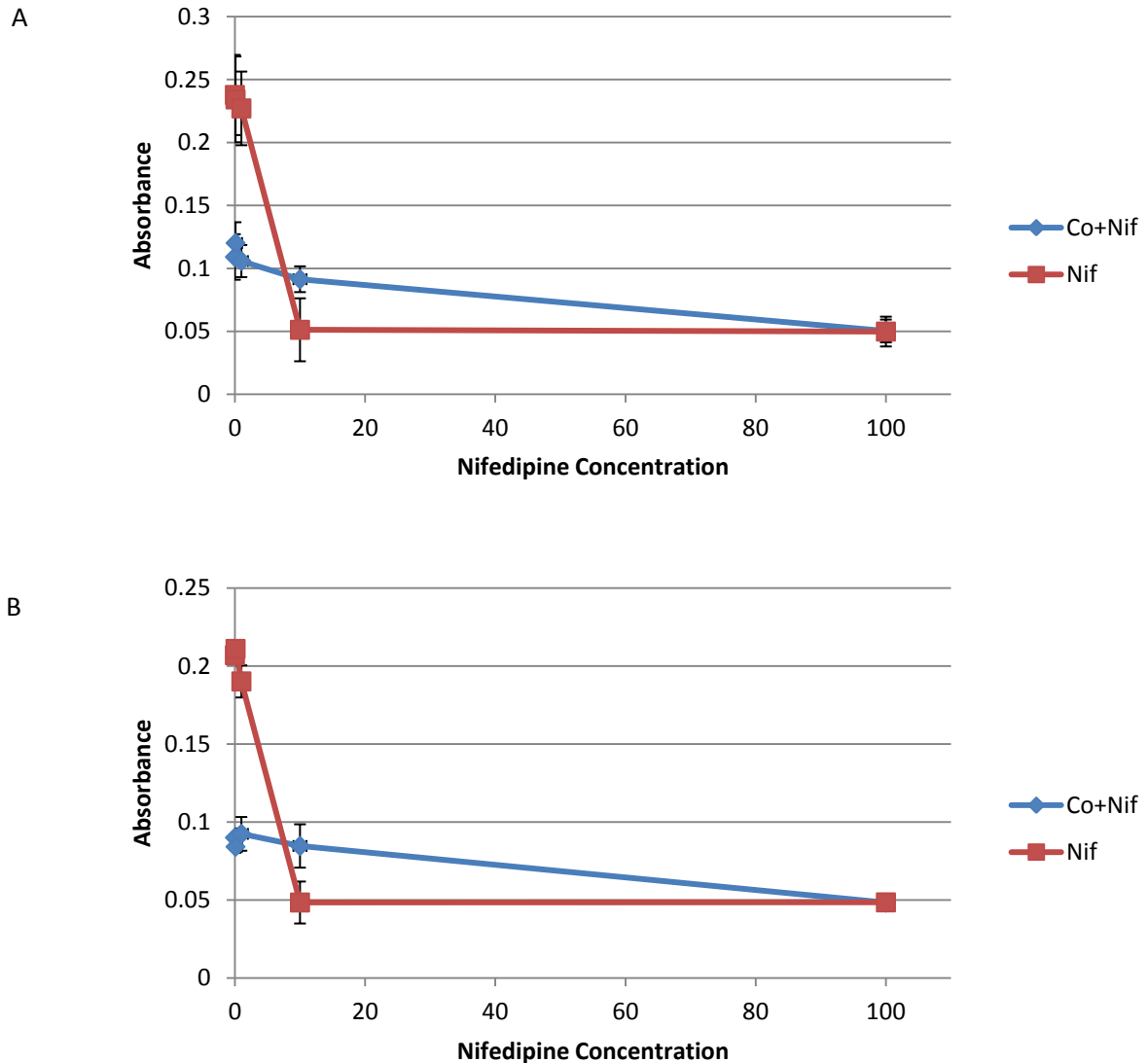
Graph 3.4: Dose response curves were plotted for nifedipine at 48 hours; viability versus the \log_{10} scale of nifedipine concentration, to obtain LD₅₀ values shown by NR (A) – 6.28 μM; and MTT (B) – 6.70 μM; n = 12.

3.2.2. Nifedipine and Cobalt (100 μ M fixed)

As with cobalt assays, a more visible decrease in NR absorbance and MTT reduction was seen at 48 hours than 24 hours post nifedipine treatment (refer to *graph 3.5*). Nifedipine shows a steady decrease in absorbance/reduction at low concentrations, before dropping dramatically at 10 μ M (potentially very toxic level, as LD₅₀ calculated at \sim 6 μ M), where it levels off and remains steady until 100 μ M. Interestingly, the error bars indicating variation between values was not as great for MTT as they had been for cobalt (see *graph 3.2*) When nifedipine was combined with cobalt, a cobalt concentration of 100 μ M was chosen, as it had shown to be cytotoxic to OST 5 cells in previous stages of the experiment, and a concentration of known toxicity was necessary, in order to investigate whether or not the calcium channel blockers would have a reducing effect on this toxicity. One-way ANOVA was again used to significantly differentiate the control group from the nifedipine-treated groups and confirm that the drug had an effect on the OST 5 cells. Significant differences were reported from the ANOVA data, and Post-hoc Fisher testing was carried out, which showed that the control, and the 0.1 and 1 μ M nifedipine-treated cell groups differed significantly from the 10 and 100 μ M groups, which did not differ from each other significantly.

When increasing concentrations of nifedipine are combined with a fixed 100 μ M concentration of cobalt, in both assays there was an increase in absorbance after the control, in the NR at 0.1 μ M and in the MTT assay at 1 μ M, before a steady dose-dependent decrease through 10 μ M to 100 μ M, where both assays reach an absorbance level of \sim 0.05. This increase could potentially mark the region in which nifedipine is exerting a therapeutic effect over the toxic effect of 100 μ M cobalt. The cobalt-nifedipine curves scores much lower on the absorbance axes initially than the nifedipine curve (100 μ M cobalt control v medium control) for NR and MTT assays, until in both assays, the nifedipine only curve drops below the cobalt-nifedipine curve at 10 μ M nifedipine, before both curves level off at the same score at 100 μ M. We concluded that nifedipine was in itself too toxic to OST 5 cells to allow us to make any conclusions about its effect on cobalt toxicity, and we

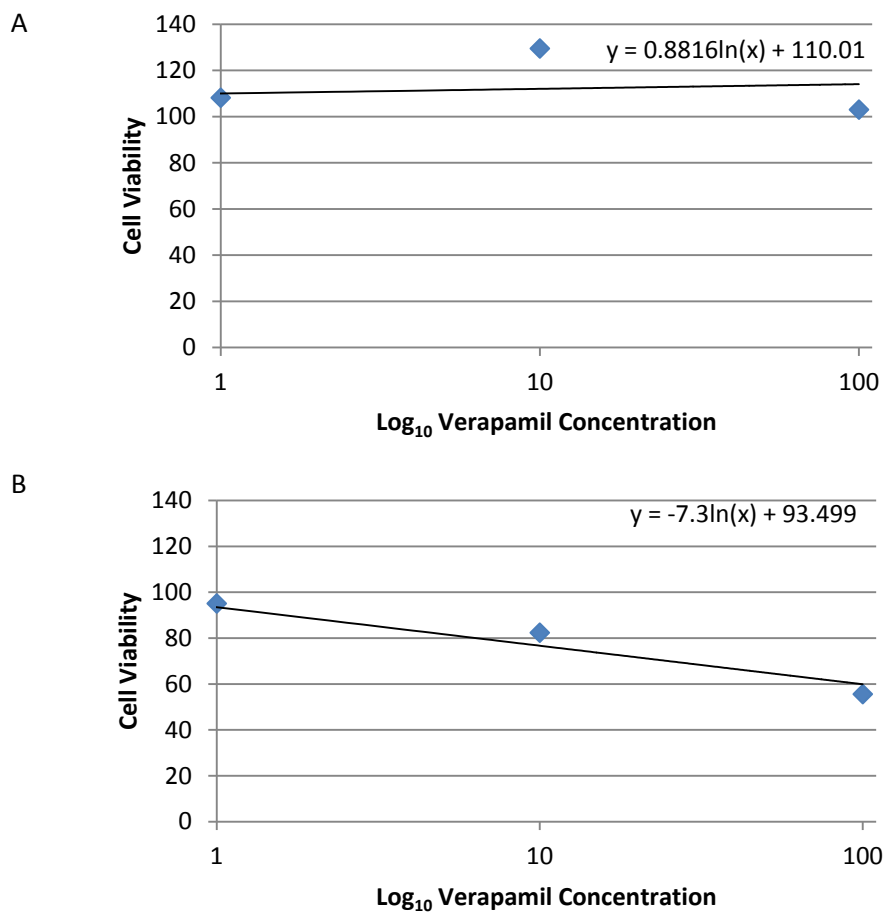
therefore changed to another calcium channel blocker, verapamil, to see was it less toxic, enabling its use with cobalt.



Graph 3.5: The effect of increasing concentrations of the calcium channel blocker nifedipine, and the effect of a fixed concentration of cobalt (100 μM) in combination with increasing concentrations of calcium channel blocker nifedipine on OST 5 cell viability at 48 hours, as shown by NR absorbance (A) and MTT reduction (B). Nifedipine was seen to decrease viability in a dose-dependent manner. Data are expressed as mean \pm SD; n = 12. Cobalt and nifedipine combined were seen to show lower viability at low concentrations, higher viability at a concentration of 10 μM nifedipine, and similar viability results at 100 μM nifedipine, than nifedipine alone. ANOVA analysis showed significant differences in the means of nifedipine-treated groups compared to controls in NR and MTT assays ($p > 0.05$). Post-hoc Fisher analysis showed that each the control, 0.1 and 1 μM cobalt-treated groups differed significantly from the 10 and 100 μM groups in the NR and MTT assays at 48 hours; CI = 95%.

3.3. Effect of Verapamil on OST 5 Viability

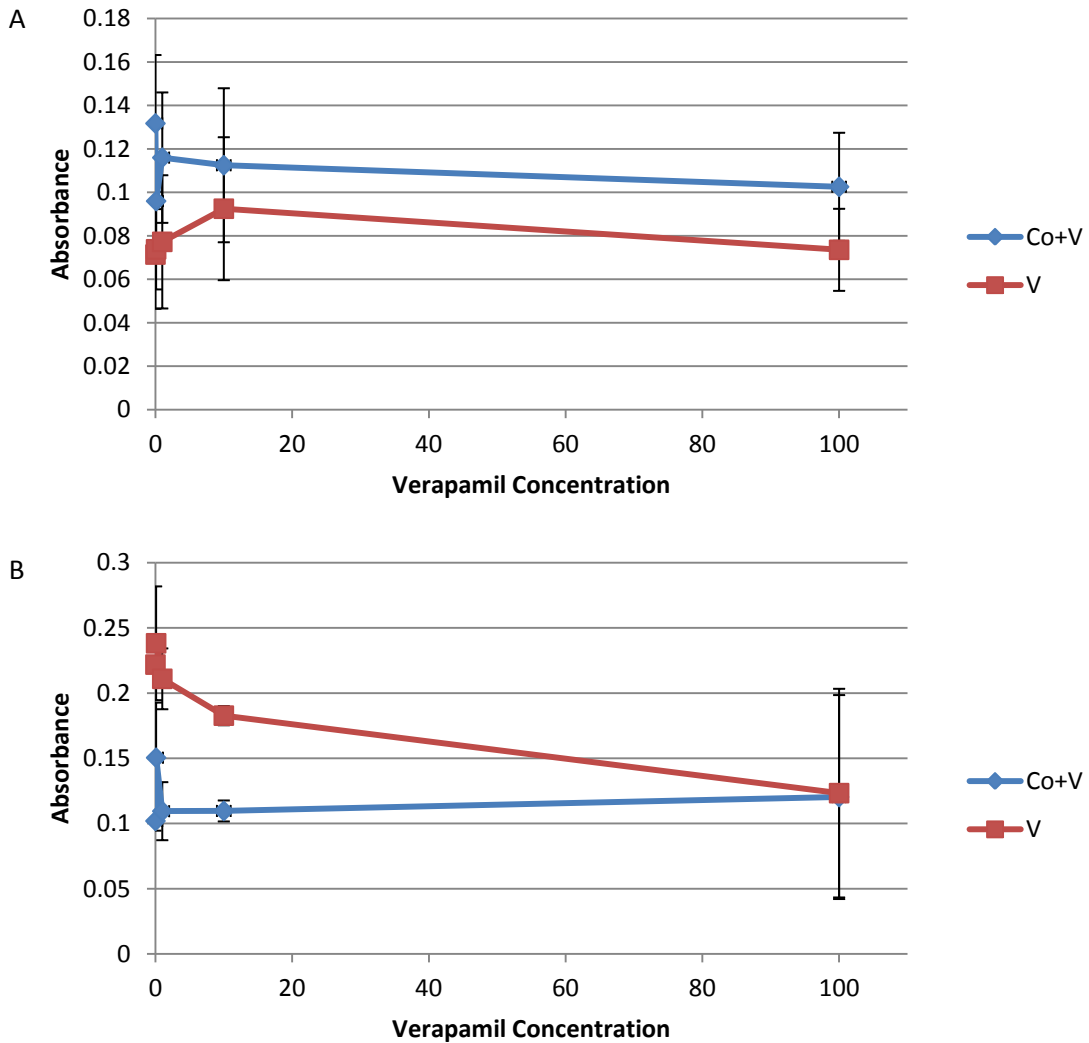
3.3.1. Verapamil



Graph 3.6: Dose response curves were plotted for verapamil at 48 hours; viability v. the log₁₀ scale of nifedipine concentration, to obtain LD₅₀ values shown by NR (A) – 3.65×10^{29} μM; and MTT (B) – 387.61 μM; n = 12.

LD₅₀ figures obtained from the verapamil NR and MTT assays were much higher at 3.65×10^{29} and 387.61 μM, respectively, than those of the nifedipine assays. Verapamil proved to be a much less toxic chemical than both cobalt and nifedipine. A higher dose of verapamil than nifedipine was therefore permitted, making it a more desirable calcium channel blocker, and it was therefore used in the further stages of this experiment.

3.3.2. Verapamil and Cobalt (100 μM fixed)



Graph 3.7: The effect of increasing concentrations of the calcium channel blocker verapamil, and the effect of a fixed concentration of cobalt (100 μM) in combination with increasing concentrations of calcium channel blocker verapamil on OST 5 cell viability at 48 hours, as shown by NR absorbance (A) and MTT reduction (B). Verapamil was seen to generally decrease absorbance in a dose-dependent manner. Data are expressed as mean \pm SD; n = 12. Cobalt and verapamil combined were seen to show similar results, slightly higher at low concentrations, to verapamil alone in the NR assay, and in the MTT assay, cobalt and verapamil showed lower viability at low verapamil concentrations than verapamil alone, but similar results were seen at concentrations of 100 μM verapamil. ANOVA analysis showed significant differences in the means of verapamil-treated groups compared to controls in MTT and NR assays ($p < 0.01$). Post-hoc Fisher analysis showed that the 10 μM verapamil-treated group differed from all other groups of the NR assay, and 100 μM verapamil-treated group differed from all other groups, as well as 0.1 and 10 μM verapamil differing significantly from each other in the MTT assay. CI = 95%.

In verapamil-treated OST 5 cells at 48 hours, the NR assay showed a steady increase in absorbance as concentration increased, with viability peaking at 10 μM verapamil before dropping down, where the 100 μM verapamil point shows a similar score to the 0.1 μM point. This would suggest that verapamil at these concentrations is non-toxic, and even appears to increase cell numbers, with 10 μM appearing the most therapeutic concentration, and this was used in further stages of this experiment in a bid to prevent cobalt-induced toxicity, without exhibiting further toxic effects to cells. However, the MTT assay at 48 hours showed slightly different results. The only concentration which exhibits higher MTT reduction than the control is at 0.1 μM , and the increase is minor. After this point, there is a steady dose-dependent decrease in reduction as verapamil concentration increases. The MTT reduction for the control and all verapamil concentrations is much higher than the NR absorbance. One-way ANOVA testing was again used to prove there were significant differences in the means of verapamil-treated cells in comparison to the control mean, and the data then underwent Post-hoc Fisher analysis which showed a significant difference between the 10 μM group in comparison with the control and all other verapamil-treated groups in the NR assay. The MTT assay showed more varied results, reporting significant differences between the 100 μM verapamil group in comparison to all other groups, and also significant difference was seen between 0.1 and 10 μM verapamil. The significance difference seen at 10 μM verapamil in the NR assay is unsurprising due to the visible peak on *graph 3.7* seen at this concentration.

When viability of cobalt and verapamil combined was assessed, the NR and MTT assays showed similar results and curves on their respective graphs. In the NR assay, there was a dose-dependent decrease in absorbance, with the exception of the 0.1 μM point, which was lower on the graph than all other concentration points. However, all points on the cobalt and verapamil curve fall above their respective points on the verapamil only curve. The MTT assay cobalt and verapamil curve displays more erratic points than the NR assay, with all verapamil concentrations exhibiting higher MTT reduction points than the control, the highest of which being

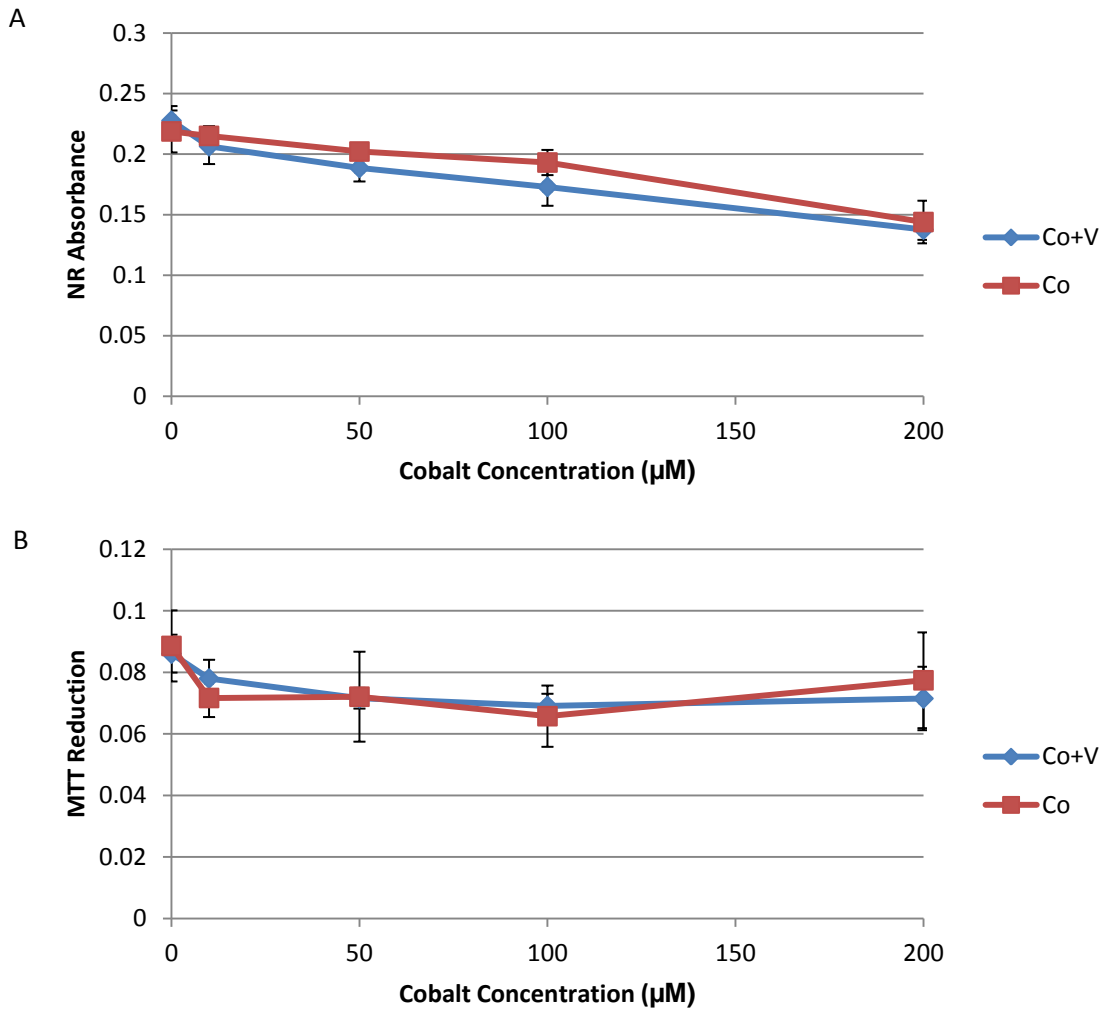
at 0.1 μM , after which it drops dramatically to a point slightly higher than that of the control for 1 and 10 μM , before rising again slightly at 100 μM . Again, all points on the cobalt and verapamil curve fall above those of the verapamil only curve, with the exception of the 100 μM point, where absorbance of both curves were very similar.

3.3.3. Verapamil (10 μM fixed) and Cobalt

In the final stage of the experiment, a concentration of 10 μM verapamil was used as it showed, in a previous MTT assay of this experiment, a non-toxic, and potential calcium channel-blocking effect on the OST 5 cells. It was decided that this was the verapamil concentration at which the drug was most likely to have a reducing effect on the cytotoxicity caused to the OST 5 cells by cobalt, which was administered in increasing doses, in an attempt to investigate the interaction with verapamil.

At 24 hours, the NR assay shows general dose-dependent decreases in absorbance in both the combined cobalt-verapamil group and the cobalt-treated group. Independent 2-sample Students' t-tests were carried out to compare absorbance levels at every concentration of cobalt between the two groups, and significant differences were seen at 50 and 100 μM in this NR assay. All points on the cobalt only curve fall above those on the cobalt and verapamil curve, besides the control. In the MTT assay, the effect of cobalt on absorbance was more erratic than the NR assay and it did not appear to represent a dose-dependent decrease in cell viability, as at 10 and 200 μM , absorbance was higher than at their respective previous points on the curve. Also, in this assay, two points of the cobalt only curve lay below the corresponding points of the cobalt and verapamil curve, 10 and 100 μM . The cobalt and verapamil curve of the MTT assay followed a dose-dependent MTT reduction decrease similar to the one seen in absorbance in the NR assay, with the exception of the 200 μM point, which has a higher reduction than at 100 μM . Independent 2-sample Student's t-tests showed significance between the two

groups at only 10 μM cobalt. All points on the MTT assay graph were much lower than the points on the NR assay graph.

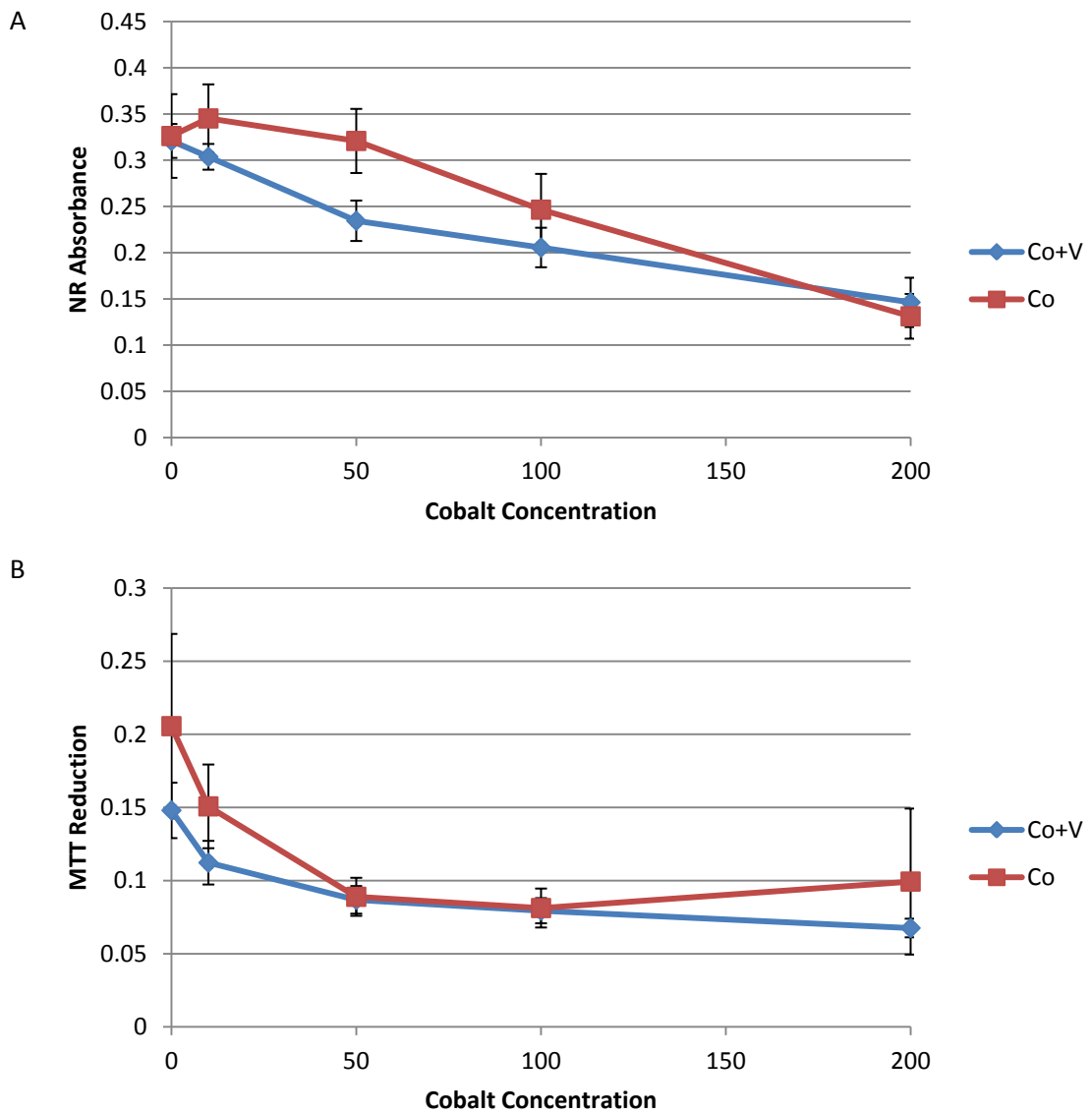


Graph 3.8: The effect of cobalt on the viability of OST 5 cells when combined with a fixed concentration of calcium channel blocker verapamil (10 μM) at 24 hours, shown by NR (A) and MTT (B) assays. Data are expressed as mean \pm SD; n = 12. Independent 2-sample Students t-tests showed significance at 50 and 100 μM in NR and at 10 μM in MTT; $p > 0.05$.

At 48 hours, the NR and MTT assays exhibited similar results to the assays at 24 hours. All points on the cobalt curve in the NR assay fall above those on the cobalt and verapamil curve, with the exception of the 200 μM mark. Significance was

shown by t-test between the cobalt and cobalt-verapamil groups at cobalt concentrations of 10, 50 and 100 μM . The cobalt generally follows a dose-dependent decrease pattern, but at 1 μM , the absorbance is higher than the control. The cobalt and verapamil curve follows an obvious dose dependent pattern, which can be likened to the same curve at 24 hours. The MTT assay displays a dose-dependent decrease in MTT reduction in the cobalt and verapamil curve, and also in the cobalt only curve, with the exception of the last point, which shows an increase from the previous point. Students t-test found significance between the two treatment groups at 10 and 200 μM . Again, most points of the cobalt curve fall above the corresponding points of the cobalt and verapamil curve.

According to the results from these viability assays, and the graphs constructed from the results, the addition of a fixed concentration of verapamil (10 μM) to increasing concentrations of cobalt does not significantly raise the NR absorbance or MTT reduction of the OST 5 cells, in comparison to cells treated with only cobalt. Therefore, the verapamil does not appear to prevent the cobalt-induced cytotoxicity observed in this experiment.



Graph 3.9: The effect of cobalt on the viability of OST 5 cells when combined with a fixed concentration of calcium channel blocker verapamil (10 μM) at 48 hours, shown by NR (A) and MTT (B) assays. Data are expressed as mean±SD; n = 12. Independent 2-sample Students t-tests showed significance at 10, 50 and 100 μM cobalt (NR) and in the control and at 10 and 200 μM cobalt; $p > 0.05$.

3.4. Osteoblast Images

3.4.1. Unstained OST 5 Cell Images

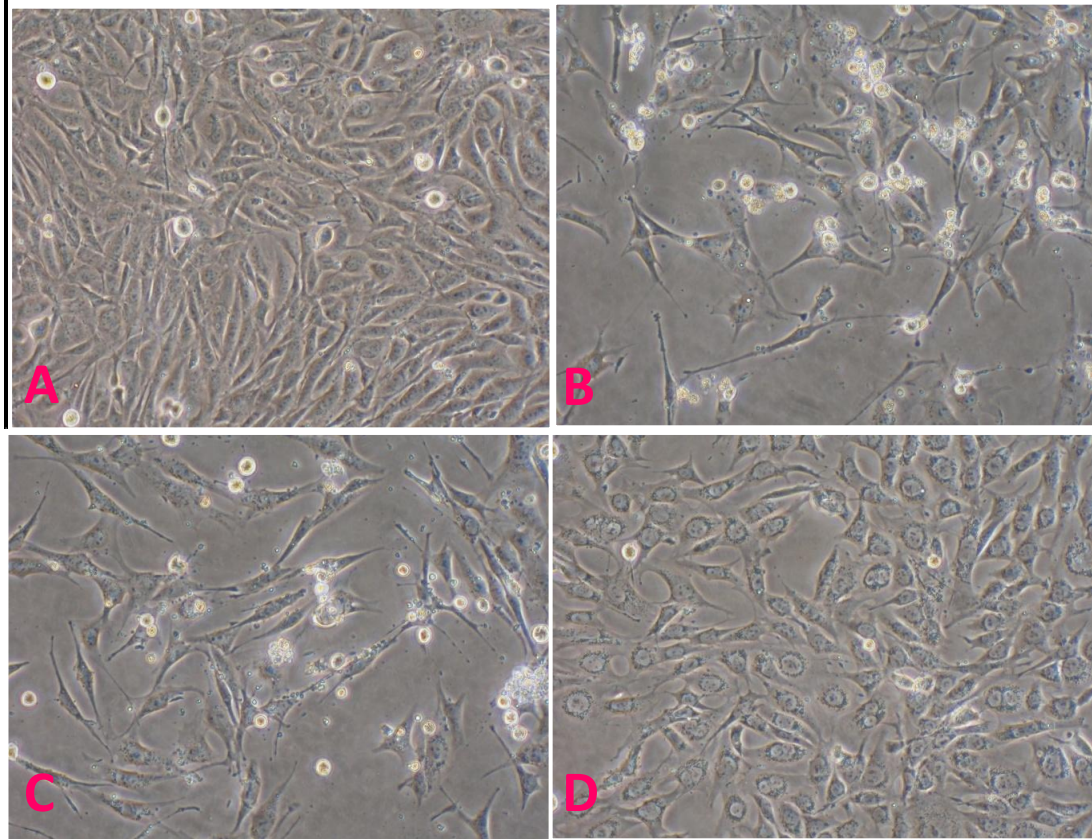


Figure 3.1: The visible effects of fixed concentrations of 10 μM verapamil (B), a combination of 100 μM cobalt and 10 μM verapamil (C) and 100 μM cobalt (D) on OST 5 cells, cultured for 24 hours, compared to a control (A) at 48 hours post-treatment. There were notable deviations in appearance of cells in all groups when compared to the control cells, but the cobalt and cobalt+verapamil treated groups bore resemblances to each other.

Images were taken of the unstained OST 5 cells under a microscope at a magnification of x200 at 48 hours post-treatment with control, 10 μM verapamil, combined 10 μM verapamil and 100 μM cobalt combined, and 100 μM cobalt. The cells appeared much less confluent in the verapamil (B), and the combined verapamil and cobalt (C) treated cells, in comparison with the control (A). There appears to be more empty space between the cells, which are aggregated in

clusters, especially in the verapamil group. There are less nuclei visible in the cobalt (D) treated cells, and the cells themselves appear much more granular than the cells of the other groups. However, the cobalt-treated image (D) appears to have less empty space between cells than in verapamil (B) and cobalt-verapamil (C) treated cells. Dose-response curves for verapamil and cobalt in this experimentation show a decrease in OST 5 cell viability for both chemicals, with the latter exhibiting a more toxic response. The reduction in living cells in the above images correlates with the reduction in living cells exhibited by the dose-response curves. However, the appearance of the cells in the verapamil (B) and cobalt-verapamil (C) treated cells suggests that verapamil has an effect on the morphology of these cells.

3.4.2. Phalloidin-FITC Stained OST 5 Cells

Cells were seeded for 24 hours before treatment, and all images were taken 48 hours post-treatment. Phalloidin-FITC staining showed visible reductions in the presence of actin in all treatment groups in comparison to the control (A). The control group showed a multidimensional presence of actin layers with few gaps. In verapamil (B) and verapamil and cobalt (C) treated cells, there is an obvious decrease in the volume of actin filaments; there appears to be less 3-dimensional layers of actin and more gaps between filaments. The actin also appears to be a brighter colour in the control group (A) when compared to group B and C. The cobalt treated (D) group displays actin much more sparsely than the control; there is very little 3D layering and there are much more gaps between filaments than in all other groups. Groups B and C seem to have a similar level of actin filaments present in these images, and cobalt-treated cells seemed to have less actin filaments present compared to cells treated with verapamil as well as cobalt. Actin filaments appear to be distributed evenly throughout all cells observed in control group and all treatment groups.

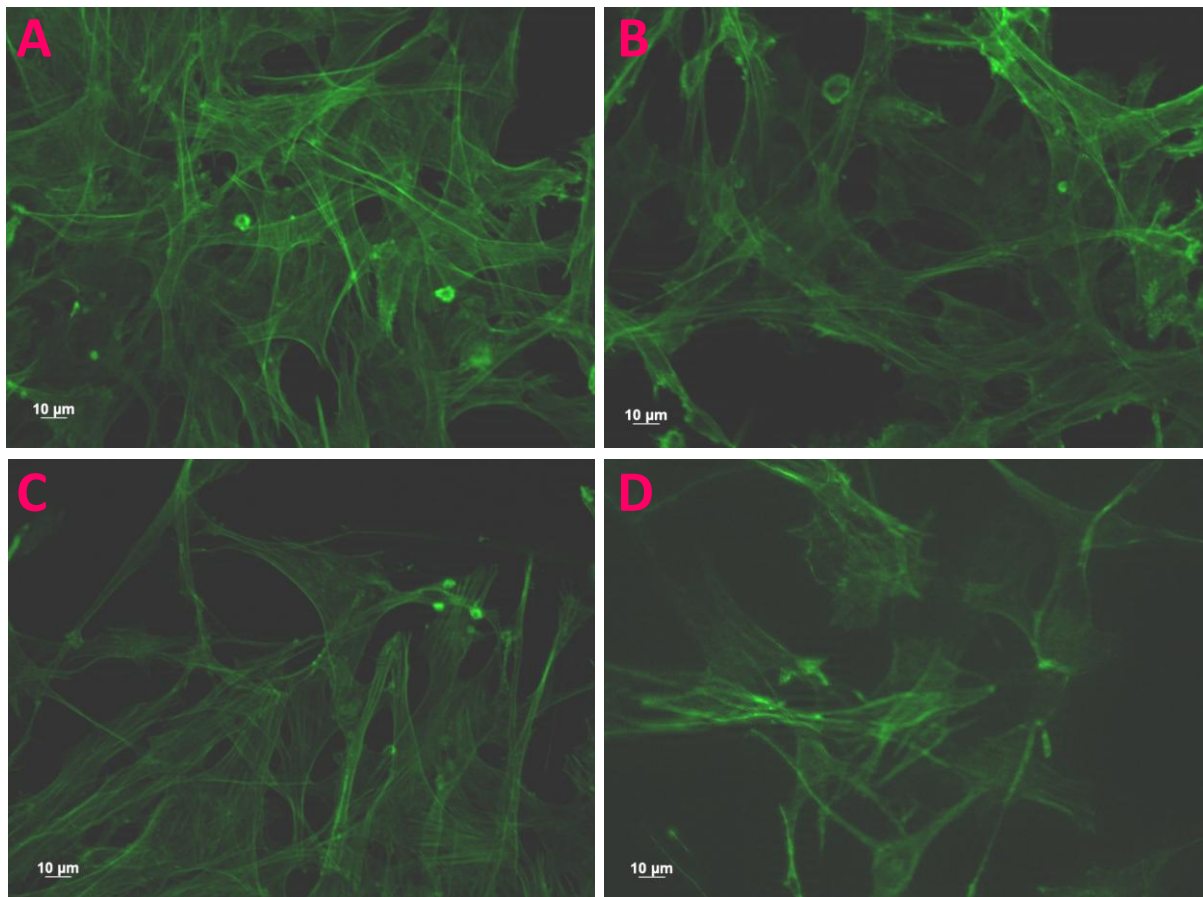


Figure 3.2: Phalloidin-FITC staining for actin on control (A), 10 μM verapamil-treated (B), 10 μM verapamil and 100 μM cobalt-treated (C) and 100 μM cobalt-treated (D) cells using fluorescence microscopy viewed at x200 with a dry lens. OST 5 cells seeded for 24 hours, treated for 48 hours.

3.4.3. Propidium Iodide (PI) and CFDA Stained OST 5 Cells

As with the phalloidin-FITC staining, cells were seeded for 24 hours before treatment, and all images were taken at 48 hours post-treatment. When cells were stained for viability with propidium iodide and CFDA, there were noticeable differences between all treatment groups in comparison to the control. The cells appear confluent in the control group (A), with very little open space between cells visible. There are similar amounts of red staining visible in both the control (A) and verapamil group (B), ~ 4 small dots, but less green staining overall is seen in group B. The verapamil-treated (B) group showed less confluence and more space

between cells, but appears to show greater cell viability than in the verapamil and cobalt-treated (C) cell group, which exhibits a greater red stain presence than either the control or the verapamil groups, along with much less green stain, which is much less bright in appearance. The cobalt-treated (D) cells seem to show very little cell viability in comparison to the control cells, with the vast majority of the image occupied with cells and very little green stain visible. There are small areas of red stain present in the cobalt group image (D), but less than in the cobalt-verapamil group (C). This staining implies that verapamil has much less of an effect on cell viability than cobalt, and the addition of verapamil to the cobalt may even increase cell viability in this case.

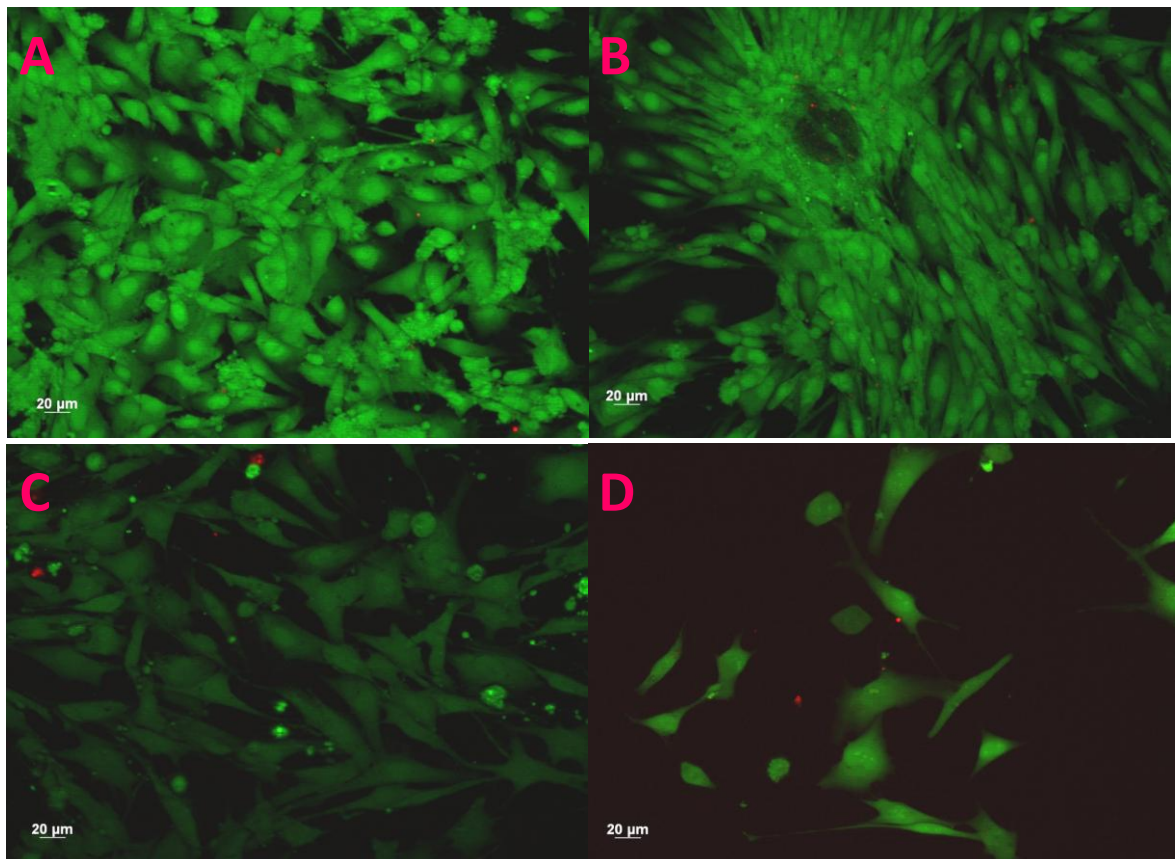


Figure 3.3: Cell viability staining using PI and CFDA on control (A), 10 μ M verapamil-treated (B), 100 μ M cobalt and 10 μ M verapamil-treated (C) and 100 μ M cobalt-treated (D) cells using confocal microscopy viewed at x200 using a wet lens. OST 5 cells were seeded for 24 hours, treated for 48 hours.

4. Discussion

This study confirmed that cobalt significantly reduced viability of OST 5 cells in a dose dependent manner. The reduced viability in NR assay is represented by decreased absorbance, indicative of damage to cell lysosomes which, when healthy, red NR dye accumulates, increasing in intensity. NR assay at 24 hours confirmed significant reduction in viability in higher cobalt concentrations ($\geq 100 \mu\text{M}$) and in concentrations $\geq 10 \mu\text{M}$ at 48 hours, which suggested that the toxic effects of cobalt were increased with incubation time. Though the MTT graphs exhibited similar curves to the NR graphs, significant differences was not seen between control cells and cobalt-treated cells in the MTT 48 hour assay, and this is most likely due to the large standard deviation in the figures of cells of each group, especially at $200 \mu\text{M}$ (*Graphs 3.1, 3.2*).

According to dose-response curves, nifedipine appeared more cytotoxic to OST 5 cells than cobalt, and was substituted by the less toxic verapamil, which displayed an LD_{50} which was of a much higher concentration than both nifedipine and cobalt. In this study, nifedipine a dose-dependent reducing effect on the OST 5 cells, exhibited by the decreased absorbance of NR and the reduction of MTT and increasing concentrations of nifedipine did not significantly alter the extent of cobalt-induced toxicity, at a fixed concentration of $100 \mu\text{M}$ cobalt, in OST 5 cells at the concentrations and time scales measured. Combined nifedipine and cobalt-treated cells showed lower absorbance figures at 10 and $100 \mu\text{M}$ nifedipine, than the $100 \mu\text{M}$ cobalt only control at 48 hours (*Graph 3.5*).

However, in *graph 3.7*, verapamil and cobalt combined have significantly higher MTT reduction at $100 \mu\text{M}$ verapamil – $100 \mu\text{M}$ cobalt, than in the control of $100 \mu\text{M}$ cobalt at 48 hours. This may suggest the involvement of verapamil and calcium channels in the alteration of the toxic effects of cobalt. However, this is not strong evidence, as it is not seen in the NR assay of the same time point. Interestingly,

there is a significant increase in absorbance at 10 μ M verapamil compared with the control and 1 μ verapamil, and this indicates an increase in cell numbers. Graph curves depicting the viability scores of 10 μ M verapamil in combination with increasing cobalt concentrations closely followed the curves of increasing concentrations of cobalt only, at 24 and 48 hours (*Graphs 3.8, 3.9*). Though significance was seen between groups of the cobalt-treated and verapamil and cobalt-treated graphs at various concentrations of cobalt, the vast majority of this significance indicated that cobalt-treated cells exhibited higher absorbance levels than verapamil and cobalt-treated cells, in both MTT and NR assays at 24 and 48 hours. Therefore, there was no significant evidence seen in these viability assays that the calcium channel blocker verapamil had a limiting effect on the toxicity exerted by cobalt on OST 5 cells.

Differences in NR and MTT assay viability absorbance may be due to the fact that, though both a capable demonstrator of viability, they work by different mechanisms; NR measures the ability of the intracellular lysosomes to bind and retain the red dye, while MTT measures the respiratory capacity of the cell. The generally-higher viability scores seen in NR assays across the experiment, in comparison to MTT viability scores, may be due to the fact that MTT is a slightly more sensitive assay in assessing toxicity regarding material as small as nanoparticle-sized (180).

Unstained OST 5 photos magnified at x200 show that cells treated with verapamil and a combination of verapamil and cobalt portray a much less confluent picture than that of the untreated, control group. The cells appear to be fewer in number, indicating that cell division has been inhibited. Cells appear less confluent in the cobalt-treated group, compared to the control, and the cells appear noticeably more granular than in all other groups. The phalloidin-FITC stained cells portray multidimensional layers of actin filaments in the control group. There is an obvious decline in 3-dimensional actin layering in verapamil, cobalt, and combined verapamil and cobalt-treated OST 5 cells, with the latter being the most affected,

displaying extremely sparse filaments. This is again most likely to be due to the cells growing less densely, with cell division having been inhibited. As the function of actin protein in the cell cytoskeleton is to provide mechanical support and aid cytoplasmic trafficking and signalling, a reduction in the presence of actin may suggest less viable cells are present, and that proliferation may have been altered by the cobalt, and the verapamil and cobalt-verapamil combination in the other groups. There is no evidence to suggest apoptosis occurs in these OST 5 cells. In apoptotic cells, actin moves to encircle the cell membrane, making it stronger so that cell contents do not leak out, and this does not appear to occur in these images.

Viability testing with propidium iodide and CFDA exhibited similar results in control and verapamil-treated cells, where there is much green stain visible, suggesting confluent and viable cells. Verapamil and cobalt treated cell images appear less confluent than control cell images, where more space can be seen between cells. Cobalt-treated cells appear to have decreased substantially in number compared to the control. Very little cells can be seen in this image. Distinctive loss of membrane integrity cannot be seen in these pictures, which is a reason apoptosis would be suspected as a method of cell death here over necrosis. PI has become a widely-used method of evaluating apoptosis in cells, relying on the fact that apoptotic cells are characterized partly by DNA fragmentation, and this chemical binds to and labels DNA, making it possible to analyse cellular DNA content (181). A TUNEL assay would be another method by which to further confirm or deny the incidence of apoptosis in these cells. However, the cells do not appear to be withdrawing from each other, which is a classic indication of apoptosis. Also, there is a lack of red staining seen in these images here, and combined with the dwindling concentrations of green staining this may suggest that, rather than being responsible for cell death, the cobalt may be affecting and perhaps halting cell proliferation, resulting in a reduced number of cells, without an increased occurrence of cell death. MTT and NR assays support this theory also, with viability assays measure a decrease in viability, not necessarily cell death, and a reduction in viable cells could be responsible for the decreases seen in NR absorbance and MTT

reduction in this project. Also, cobalt-treated cells appeared less confluent than control cells at 48 hours when examined under microscope in well plates prior to viability assays being carried out.

4.1. Are Calcium Channels Involved?

It would appear from the results obtained in this experiment that cobalt does not exert its toxic effects via L-type voltage-dependent calcium channels (VDCCs). However, there is not enough conclusive evidence present here to completely eradicate the theory, based on the viability assay results seen following the addition of the calcium channel blockers. One would envisage that had calcium channels been involved in the toxicity seen in these OST 5 cells, their blockage would be sufficient to significantly reduce the effects of cobalt, thus increasing the viability scores seen in NR and MTT assays, which failed to occur. Previous experimentation has suggested that at concentrations of 10 μM , verapamil has inhibited cellular processes in osteoblasts believed to be governed by L-type voltage-gated calcium channels (175) and, at concentrations of as low as 1.5 μM , verapamil has prevented a PTH-induced increase in free cytosolic calcium by 50% (176).

However, sufficient steps to ensure verapamil had completely blocked all calcium channels at a dose of 10 μM were not taken in this experiment. Also, had the calcium channels been adequately obstructed by verapamil, would it be possible for cobalt to act via different channels? It would be beneficial to investigate the effects of cobalt on alternative entry routes into osteoblasts, and ultimately, other cells also.

Further investigation must be carried out to help clarify the results seen here, and help further elucidate the relationship between calcium channels and cobalt toxicity. Firstly, Ca^{2+} regulation could be monitored in cells, to ensure that verapamil and nifedipine were adequately obstructing calcium channels at the concentrations used. Calcium imaging is carried out by fluorescent protein indicators which can

chelate calcium ions. The fluorescent dye Fura-2, a pentacarboxylate calcium indicator developed in the 1970s, is considered the most popular fluorescent cytosolic calcium probe (182), allowing the monitoring of the free cytosolic concentration of calcium, $[Ca^{2+}]_i$, in living cells. Fura-2-acetoxymethyl ester (Fura-2AM) is the membrane-permeable derivative of Fura-2, which regenerates into Fura-2 once diffused into cells when cellular esterases remove the acetoxymethyl ester group. Fura-2 becomes excited at 340 – 380 nm of light, and the emissions at these wavelengths directly correspond to the amount of intracellular calcium present. If the calcium channel blockers used in this experiment were sufficient in their concentrations, $[Ca^{2+}]_i$ would be lower in verapamil/nifedipine treated groups in comparison to the control group.

Another method by which to assess the adequacy of the calcium channel blockers would be to introduce a calcium channel agonist, and investigate whether the actions of the agonist were revoked by the concentrations of the antagonists, verapamil and nifedipine, used in this experiment. Bay K8644 is a known L-type voltage-gated calcium channel agonist. This chemical is primarily used experimentally in this manner, and has been known to increase $[Ca^{2+}]_i$ in a concentration-dependent manner in osteoblasts (163) and human oral cancer cells (OC2) (183). Bay K8644 has also stimulated the secretion of bone matrix protein osteocalcin in osteoblast-like osteosarcoma cells, and increases bone creation and bone resorption (184); the resorption seen was impeded by desmethoxyverapamil, a verapamil type radioligand developed for studying calcium channels (185). This Bay K8644-induced Ca^{2+} influx has also previously been blocked by nifedipine (183). If, at the concentrations used in this study, the increase of $[Ca^{2+}]_i$ is blocked, the nifedipine and verapamil would be considered to have impeded the action of Bay K8644, and are therefore sufficient in these concentrations as calcium channel antagonists.

4.3. Alternative Materials in Total Hip Arthroplasty

Due to the recent adverse attention commanded by the use of metal in hip prosthetics, and the ongoing pursuit to develop the most inert and compliant implant possible for human use, other materials are continually being assessed and considered for clinical application. Presently, there exists no faultless alternative material to cobalt chromium for use in THA; there are pros and cons associated with every potential substance.

4.3.1. Ceramics

Alumina ceramic (Al_2O_3) is an example of one such material, investigated due to its reported good performance as a bearing material in terms of annual wear (89, 186, 187). However, to avoid excessive wear, extreme care must be taken during the positioning of the device (188), and impingement at the femoral neck can lead to wear and osteolysis (189). Less volumetric wear is believed to occur over time in ceramic on ceramic (CC) implants, rather than MM, as alumina is a harder material (i.e. Young's modulus is higher) (190, 191), but more, smaller particles are expected to be released from the former (192). There is little known about the accumulation of alumina ceramic wear debris in the periprosthetic tissue and its effect *in vivo*, in comparison to what is known about MM and MP wear debris and its effects. The potential effects of these particles on cells must be determined in order to establish the probable long-term effects of the generation of these particles *in vivo*. In a study using histiocytes and fibroblasts, Germain *et al*, 2002, found Al_2O_3 particles to be toxic in nanoparticle size, possibly due to the lowering at this size in the oxidation state of alumina, which is usually stable in large particles. However, these particles were still seen to be less cytotoxic than CoCr particles in this study (89).

Zirconia ceramic was proposed to be tougher, with improved wear properties, than alumina ceramic (193). But the case studies investigated in this paper did not put to rest the concerns of ceramic being a brittle substance that can break, and the improved zirconia ceramic could not eliminate the incidence of catastrophic

breakage. The dilemma with these devices involves choosing low wear ceramic, which carry a risk of fracture, or higher wear cobalt-chromium, which will not fracture. Hummer *et al*, 1996, recommended a return to cobalt-chromium as the material of choice given all the information available at the time (193). Park *et al*, 2006, also recommended discontinued use of alumina ceramic, due to catastrophic breakage, and an audible squeaking noise has been reported with CC implants, which could irritate the patient (194, 195).

4.3.2. Titanium

Titanium alloys are strong and excellently tolerated by the body, and have long since been used successfully in dental implants. However, despite desirable mechanical characteristics, they exhibit a low resistance to wear. Titanium alloys are used in THA, not as the articulating surface, but as the stem component, coupled with a femoral head constructed from another material in order to avoid the titanium stem being subjected to abrasion and rubbing. An attractive characteristic of titanium is its elasticity; an elastic stem can evenly distribute and transport stresses applied from the body's weight through the whole stem. Corrosion of the titanium stem is also rare, due to passivation by titanium oxide (196). However, these implants are not without their problems, as intractable pain and crevice corrosion leading to cortical hypertrophy have been reported in association with titanium stems (196).

4.4. What's Next for Cobalt-Chromium in THA?

Cobalt was the focal point of this experiment, rather than chromium, due to its ability to enter cells quickly and be transported readily to all organs of the body, indicating great potential for widespread systemic damage. Higher circulating levels of cobalt ions than chromium also indicate the implications cobalt has for adverse

systemic effects in patients, as well as the local damage it has been seen to cause in the periprosthetic area of MM THA and HR patients.

While it is insisted that patients with CoCr hip prostheses who experience such adverse effects outlined in this study are in the extreme minority, with a process that is being carried out at such an increasing rate worldwide and one which is vital to the treatment of osteoporosis, any related adverse reaction encountered must be regarded a cause of concern and investigated thoroughly. The results observed in this experiment draw parallels with previous work, whether or not the effects are mediated via calcium channels, using these concentrations of cobalt in lymphocytes (197) and human osteoblast-like SaSO-2 cells (177).

4.4.1. Infection Control

Another method to potentially reduce need for revision in MM THA and HR is to attempt to prevent the development of infection, which has previously been cited as a main reason for implant failure. Emerging antibiotic-resistant strains of common bacteria pose a serious problem for MM implants and implant-related infections. Though the percentage of patients who develop implant-associated infections is low, the procedure is gaining popularity, so there is a demand for new methods of preventing these infections. A recent article in Nature magazine (April 2012) discussed mechanisms for the controlled release of antimicrobials at the site of implant. These included the administration of a matrix, serving as a depot for antimicrobial agents, with the implant, antimicrobial coatings on titanium components to prevent intramedullary infection, the use of the antimicrobial silver ion for incorporation into pre-coated implants, and fatty acid cis-2-deconoic acid (C2DA) has shown the potential to prevent biofilm formation, and disrupt pre-existing biofilms (198), which may be beneficial as targeting infections established in biofilms is difficult (199).

Further research must be devoted to elucidating how cobalt operates at a cellular level and every mechanism by which it elicits its toxic systemic and local tissue effects. When a further understanding of cobalt is obtained, investigation can be carried out into eradicating all adverse cobalt-induced reactions, particularly wear, loosening, and osteolysis, the three dominant concerns recognised in THA, while still utilising cobalt-chromium MM prostheses.

References

1. Gomez PF, Morcuende JA. Early attempts at hip arthroplasty--1700s to 1950s. *Iowa Orthop J.* 2005;25:25-9. PubMed PMID: 16089067. Pubmed Central PMCID: 1888777. Epub 2005/08/11. eng.
2. The classic. Metal hip joint. A case report. By Austin T. Moore and Harold R. Bohlman. 1943. *Clin Orthop Relat Res.* 1983 Jun(176):3-6. PubMed PMID: 6342894. Epub 1983/06/01. eng.
3. Wroblewski BM. Professor Sir John Charnley (1911–1982). *Rheumatology.* 2002;41(7):824-5.
4. Huo MH, Parvizi J, Bal BS, Mont MA. What's new in total hip arthroplasty. *J Bone Joint Surg Am.* 2009 Oct;91(10):2522-34. PubMed PMID: 19797590. Epub 2009/10/03. eng.
5. Sibanda N, Copley LP, Lewsey JD, Borroff M, Gregg P, MacGregor AJ, et al. Revision Rates after Primary Hip and Knee Replacement in England between 2003 and 2006. *PLoS Med.* 2008;5(9):e179.
6. Daniel J, Pynsent PB, McMinn DJ. Metal-on-metal resurfacing of the hip in patients under the age of 55 years with osteoarthritis. *J Bone Joint Surg Br.* 2004 Mar;86(2):177-84. PubMed PMID: 15046429. Epub 2004/03/30. eng.
7. Girard J, Lavigne M, Vendittoli PA, Roy AG. Biomechanical reconstruction of the hip: a randomised study comparing total hip resurfacing and total hip arthroplasty. *J Bone Joint Surg Br.* 88. England2006. p. 721-6.
8. Little JP, Taddei F, Viceconti M, Murray DW, Gill HS. Changes in femur stress after hip resurfacing arthroplasty: Response to physiological loads. *Clinical biomechanics (Bristol, Avon).* 2007;22(4):440-8.
9. Kishida Y, Sugano N, Nishii T, Miki H, Yamaguchi K, Yoshikawa H. Preservation of the bone mineral density of the femur after surface replacement of the hip. *J Bone Joint Surg Br.* 2004 Mar;86(2):185-9. PubMed PMID: 15046430. Epub 2004/03/30. eng.
10. Ball ST, Le Duff MJ, Amstutz HC. Early results of conversion of a failed femoral component in hip resurfacing arthroplasty. *J Bone Joint Surg Am.* 2007 Apr;89(4):735-41. PubMed PMID: 17403794. Epub 2007/04/04. eng.
11. Vassiliou K, Scholes SC, Unsworth A. Laboratory studies on the tribology of hard bearing hip prostheses: ceramic on ceramic and

metal on metal. Proc Inst Mech Eng H. 2007 Jan;221(1):11-20. PubMed PMID: 17315764. Epub 2007/02/24. eng.

12. Bell RS, Schatzker J, Fornasier VL, Goodman SB. A study of implant failure in the Wagner resurfacing arthroplasty. J Bone Joint Surg Am. 1985 Oct;67(8):1165-75. PubMed PMID: 3902844. Epub 1985/10/01. eng.

13. Head WC. Wagner surface replacement arthroplasty of the hip. Analysis of fourteen failures in forty-one hips. J Bone Joint Surg Am. 1981 Mar;63(3):420-7. PubMed PMID: 7204442. Epub 1981/03/01. eng.

14. McKellop H, Park S-H, Chiesa R, Doorn P, Lu B, Normand P, et al. In Vivo Wear of 3 Types of Metal on Metal Hip Prostheses During 2 Decades of Use. Clinical Orthopaedics and Related Research. 1996;329.

15. Howie DW, McCalden RW, Nawana NS, Costi K, Pearcy MJ, Subramanian C. The Long-Term Wear of Retrieved McKee-Farrar Metal-on-Metal Total Hip Prostheses. The Journal of arthroplasty. 2005;20(3):350-7.

16. Mabilieu G, Kwon Y-M, Pandit H, Murray DW, Sabokbar A. Metal-on-metal hip resurfacing arthroplasty: A review of periprosthetic biological reactions. Acta Orthopaedica. 2008 2008/01/01;79(6):734-47.

17. Treacy RBC, McBryde CW, Pynsent PB. Birmingham hip resurfacing arthroplasty. Journal of Bone & Joint Surgery, British Volume. 2005;87-B(2):167-70.

18. Heilpern GN, Shah NN, Fordyce MJ. Birmingham hip resurfacing arthroplasty: a series of 110 consecutive hips with a minimum five-year clinical and radiological follow-up. J Bone Joint Surg Br. 90. England 2008. p. 1137-42.

19. MacDonald SJ, McCalden RW, Chess DG, Bourne RB, Rorabeck CH, Cleland D, et al. Metal-on-metal versus polyethylene in hip arthroplasty: a randomized clinical trial. Clin Orthop Relat Res. 2003 Jan(406):282-96. PubMed PMID: 12579029. Epub 2003/02/13. eng.

20. Sieber HP, Rieker CB, Kottig P. Analysis of 118 second-generation metal-on-metal retrieved hip implants. J Bone Joint Surg Br. 1999 Jan;81(1):46-50. PubMed PMID: 10068001. Epub 1999/03/06. eng.

21. Andrews RE, Shah KM, Wilkinson JM, Gartland A. Effects of cobalt and chromium ions at clinically equivalent concentrations after metal-on-metal hip replacement on human osteoblasts and

- osteoclasts: implications for skeletal health. *Bone*. 2011 Oct;49(4):717-23. PubMed PMID: 21689801. Epub 2011/06/22. eng.
22. Campbell P, Doorn P, Dorey F, Amstutz HC. Wear and morphology of ultra-high molecular weight polyethylene wear particles from total hip replacements. *Proc Inst Mech Eng H*. 1996;210(3):167-74. PubMed PMID: 8885653. Epub 1996/01/01. eng.
23. Purdue PE, Koulouvaris P, Potter HG, Nestor BJ, Sculco TP. The Cellular and Molecular Biology of Periprosthetic Osteolysis. *Clinical Orthopaedics and Related Research*. 2007;454.
24. Harris WH. Wear and Periprosthetic Osteolysis: The Problem. *Clinical Orthopaedics and Related Research*. 2001;393.
25. Purdue PE, Koulouvaris P, Nestor BJ, Sculco TP. The central role of wear debris in periprosthetic osteolysis. *HSS J*. 2006 Sep;2(2):102-13. PubMed PMID: 18751821. Pubmed Central PMCID: 2488166. Epub 2008/08/30. eng.
26. Archibeck MJ, Jacobs JJ, Black J. Alternate Bearing Surfaces in Total Joint Arthroplasty: Biologic Considerations. *Clinical Orthopaedics and Related Research*. 2000;379.
27. Charnley J. The long-term results of low-friction arthroplasty of the hip performed as a primary intervention. *J Bone Joint Surg Br*. 1972 Feb;54(1):61-76. PubMed PMID: 5011747. Epub 1972/02/01. eng.
28. Fisher J, Jin Z, Tipper J, Stone M, Ingham E. PRESIDENTIAL GUEST LECTURE: Tribology of Alternative Bearings. *Clinical Orthopaedics and Related Research*. 2006;453.
29. Naudie D, Roeder CP, Parvizi J, Berry DJ, Eggli S, Busato A. Metal-on-metal versus metal-on-polyethylene bearings in total hip arthroplasty: A matched case-control study. *The Journal of Arthroplasty*. 2004;19(7, Supplement 2):35-41.
30. Bizot P, Nizard R, Hamadouche M, Hannouche D, Sedel L. Prevention of wear and osteolysis: alumina-on-alumina bearing. *Clin Orthop Relat Res*. 2001 Dec(393):85-93. PubMed PMID: 11764375. Epub 2002/01/05. eng.
31. Atienza C, Jr., Maloney WJ. Highly cross-linked polyethylene bearing surfaces in total hip arthroplasty. *J Surg Orthop Adv*. 2008 Spring;17(1):27-33. PubMed PMID: 18284901. Epub 2008/02/21. eng.

32. Chan FW, Bobyn JD, Medley JB, Krygier JJ, Tanzer M. Wear and Lubrication of Metal-on-Metal Hip Implants. *Clinical Orthopaedics and Related Research*. 1999;369.
33. Medley JB, Chan FW, Krygier JJ, Bobyn JD. Comparison of Alloys and Designs in a Hip Simulator Study of Metal on Metal Implants. *Clinical Orthopaedics and Related Research*. 1996;329.
34. Glant TT, Jacobs JJ, Molnár G, Shanbhag AS, Valyon M, Galante JO. Bone resorption activity of particulate-stimulated macrophages. *Journal of Bone and Mineral Research*. 1993;8(9):1071-9.
35. Shanbhag AS, Jacobs JJ, Black J, Galante JO, Glant TT. Human monocyte response to particulate biomaterials generated in vivo and in vitro. *Journal of Orthopaedic Research*. 1995;13(5):792-801.
36. Yao J, Glant TT, Lark MW, Mikecz K, Jacobs JJ, Hutchinson NI, et al. The potential role of fibroblasts in periprosthetic osteolysis: Fibroblast response to titanium particles. *Journal of Bone and Mineral Research*. 1995;10(9):1417-27.
37. Schmalzried TP, Peters PC, Maurer BT, Bragdon CR, Harris WH. Long-duration metal-on-metal total hip arthroplasties with low wear of the articulating surfaces. *The Journal of Arthroplasty*. 1996;11(3):322-31.
38. Merritt K, Brown SA. Distribution of Cobalt Chromium Wear and Corrosion Products and Biologic Reactions. *Clinical Orthopaedics and Related Research*. 1996;329.
39. Jacobs JJ, Skipor AK, Doorn PF, Campbell P, Schmalzried TP, Black J, et al. Cobalt and chromium concentrations in patients with metal on metal total hip replacements. *Clin Orthop Relat Res*. 1996 Aug(329 Suppl):S256-63. PubMed PMID: 8769339. Epub 1996/08/01. eng.
40. Anwar HA, Aldam CH, Visuvanathan S, Hart AJ. The effect of metal ions in solution on bacterial growth compared with wear particles from hip replacements. *J Bone Joint Surg Br*. 2007 Dec;89(12):1655-9. PubMed PMID: 18057369. Epub 2007/12/07. eng.
41. Shimmin AJ, Back D. Femoral neck fractures following Birmingham hip resurfacing: a national review of 50 cases. *J Bone Joint Surg Br*. 2005 Apr;87(4):463-4. PubMed PMID: 15795193. Epub 2005/03/30. eng.
42. Steffen RT, Foguet PR, Krikler SJ, Gundle R, Beard DJ, Murray DW. Femoral neck fractures after hip resurfacing. *J Arthroplasty*.

2009 Jun;24(4):614-9. PubMed PMID: 18555654. Epub 2008/06/17. eng.

43. Amstutz HC, Beaulé PE, Dorey FJ, Le Duff MJ, Campbell PA, Gruen TA. Metal-on-metal hybrid surface arthroplasty: two to six-year follow-up study. *J Bone Joint Surg Am.* 2004 Jan;86-A(1):28-39. PubMed PMID: 14711942. Epub 2004/01/09. eng.

44. Lavigne M, Masse V, Girard J, Roy AG, Vendittoli PA. [Return to sport after hip resurfacing or total hip arthroplasty: a randomized study]. *Rev Chir Orthop Reparatrice Appar Mot.* 2008 Jun;94(4):361-7. PubMed PMID: 18555862. Epub 2008/06/17. Activites sportives apres resurfacement et prothese totale de hanche : une etude prospective randomisee. fre.

45. Willert HG, Buchhorn GH, Fayyazi A, Flury R, Windler M, Koster G, et al. Metal-on-metal bearings and hypersensitivity in patients with artificial hip joints. A clinical and histomorphological study. *J Bone Joint Surg Am.* 2005 Jan;87(1):28-36. PubMed PMID: 15637030. Epub 2005/01/08. eng.

46. Pandit H, Glyn-Jones S, McLardy-Smith P, Gundle R, Whitwell D, Gibbons CL, et al. Pseudotumours associated with metal-on-metal hip resurfacings. *J Bone Joint Surg Br.* 2008 Jul;90(7):847-51. PubMed PMID: 18591590. Epub 2008/07/02. eng.

47. Fried M, Hainer V, Basdevant A, Buchwald H, Deitel M, Finer N, et al. Inter-disciplinary European guidelines on surgery of severe obesity. *Int J Obes.* 2007;31(4):569-77.

48. Berton C, Girard J, Krantz N, Migaud H. The Durom large diameter head acetabular component: early results with a large-diameter metal-on-metal bearing. *J Bone Joint Surg Br.* 2010 Feb;92(2):202-8. PubMed PMID: 20130309. Epub 2010/02/05. eng.

49. Haddad FS, Thakrar RR, Hart AJ, Skinner JA, Nargol AV, Nolan JF, et al. Metal-on-metal bearings: the evidence so far. *J Bone Joint Surg Br.* 2011 May;93(5):572-9. PubMed PMID: 21511920. Epub 2011/04/23. eng.

50. Queally JM, Devitt BM, Butler JS, Malizia AP, Murray D, Doran PP, et al. Cobalt ions induce chemokine secretion in primary human osteoblasts. *J Orthop Res.* 2009 Jul;27(7):855-64. PubMed PMID: 19132727. Epub 2009/01/10. eng.

51. Alsema R, Deutman R, Mulder TJ. Stanmore total hip replacement. A 15- to 16-year clinical and radiographic follow-up. *J Bone Joint Surg Br.* 1994 Mar;76(2):240-4. PubMed PMID: 8113284. Epub 1994/03/01. eng.

52. Malchau H, Herberts P, Ahnfelt L. Prognosis of total hip replacement in Sweden. Follow-up of 92,675 operations performed 1978-1990. *Acta Orthop Scand.* 1993 Oct;64(5):497-506. PubMed PMID: 8237312. Epub 1993/10/01. eng.
53. Lie SA, Havelin LI, Furnes ON, Engesaeter LB, Vollset SE. Failure rates for 4762 revision total hip arthroplasties in the Norwegian Arthroplasty Register. *J Bone Joint Surg Br.* 2004 May;86(4):504-9. PubMed PMID: 15174543. Epub 2004/06/04. eng.
54. Smith AJ, Dieppe P, Vernon K, Porter M, Blom AW. Failure rates of stemmed metal-on-metal hip replacements: analysis of data from the National Joint Registry of England and Wales. *Lancet.* 379. England: 2012 Elsevier Ltd; 2012. p. 1199-204.
55. Catelas I, Petit A, Zukor DJ, Huk OL. Cytotoxic and apoptotic effects of cobalt and chromium ions on J774 macrophages – Implication of caspase-3 in the apoptotic pathway. *Journal of Materials Science: Materials in Medicine.* 2001;12(10):949-53.
56. Fleury C, Petit A, Mwale F, Antoniou J, Zukor DJ, Tabrizian M, et al. Effect of cobalt and chromium ions on human MG-63 osteoblasts in vitro: morphology, cytotoxicity, and oxidative stress. *Biomaterials.* 2006 Jun;27(18):3351-60. PubMed PMID: 16488005. Epub 2006/02/21. eng.
57. Rizzetti MC, Liberini P, Zarattini G, Catalani S, Pazzaglia U, Apostoli P, et al. Loss of sight and sound. Could it be the hip? *Lancet.* 2009 Mar 21;373(9668):1052. PubMed PMID: 19304018. Epub 2009/03/24. eng.
58. Mao X, Wong AA, Crawford RW. Cobalt toxicity--an emerging clinical problem in patients with metal-on-metal hip prostheses? *Med J Aust.* 2011 Jun 20;194(12):649-51. PubMed PMID: 21692725. Epub 2011/06/23. eng.
59. Shahgaldi BF, Heatley FW, Dewar A, Corrin B. In vivo corrosion of cobalt-chromium and titanium wear particles. *J Bone Joint Surg Br.* 1995 Nov;77(6):962-6. PubMed PMID: 7593115. Epub 1995/11/01. eng.
60. Disegi JA, Kennedy RL, Pilliar R. Cobalt-Base Alloys for Biomedical Application 1999.
61. Howie DW, Rogers SD, McGee MA, Haynes DR. Biologic effects of cobalt chrome in cell and animal models. *Clin Orthop Relat Res.* 1996 Aug(329 Suppl):S217-32. PubMed PMID: 8769336. Epub 1996/08/01. eng.

62. Galle P, Berry JP, Galle C. Role of alveolar macrophages in precipitation of mineral elements inhaled as soluble aerosols. *Environ Health Perspect.* 1992 Jul;97:145-7. PubMed PMID: 1396450. Pubmed Central PMCID: 1519563. Epub 1992/07/01. eng.
63. Lundborg M, Falk R, Johansson A, Kreyling W, Camner P. Phagolysosomal pH and dissolution of cobalt oxide particles by alveolar macrophages. *Environ Health Perspect.* 1992 Jul;97:153-7. PubMed PMID: 1396451. Pubmed Central PMCID: 1519542. Epub 1992/07/01. eng.
64. Case CP. Chromosomal changes after surgery for joint replacement. *J Bone Joint Surg Br.* 2001 Nov;83(8):1093-5. PubMed PMID: 11764417. Epub 2002/01/05. eng.
65. Langton DJ, Jameson SS, Joyce TJ, Webb J, Nargol AVF. The effect of component size and orientation on the concentrations of metal ions after resurfacing arthroplasty of the hip. *Journal of Bone & Joint Surgery, British Volume.* 2008;90-B(9):1143-51.
66. Kwon Y-M, Ostlere SJ, McLardy-Smith P, Athanasou NA, Gill HS, Murray DW. "Asymptomatic" Pseudotumors After Metal-on-Metal Hip Resurfacing Arthroplasty: Prevalence and Metal Ion Study. *The Journal of Arthroplasty.* 2011;26(4):511-8.
67. Grubl A, Marker M, Brodner W, Giurea A, Heinze G, Meisinger V, et al. Long-term follow-up of metal-on-metal total hip replacement. *J Orthop Res.* 2007 Jul;25(7):841-8. PubMed PMID: 17405158. Epub 2007/04/04. eng.
68. Devitt BM, Queally JM, Vioreanu M, Butler JS, Murray D, Doran PP, et al. Cobalt ions induce chemokine secretion in a variety of systemic cell lines. 2010 Dec;81(6):756-64. PubMed PMID: 21110705. eng.
69. Dunstan E, Ladon D, Whittingham-Jones P, Carrington R, Briggs TW. Chromosomal aberrations in the peripheral blood of patients with metal-on-metal hip bearings. *J Bone Joint Surg Am.* 2008 Mar;90(3):517-22. PubMed PMID: 18310701. Epub 2008/03/04. eng.
70. MacDonald SJ. Metal-on-metal total hip arthroplasty: the concerns. *Clin Orthop Relat Res.* 2004 Dec(429):86-93. PubMed PMID: 15577471. Epub 2004/12/04. eng.
71. MacDonald SJ, Brodner W, Jacobs JJ. A consensus paper on metal ions in metal-on-metal hip arthroplasties. *The Journal of Arthroplasty.* 2004;19(8, Supplement):12-6.

72. Jacobs JJ, Skipor AK, Patterson LM, Hallab NJ, Paprosky WG, Black J, et al. Metal release in patients who have had a primary total hip arthroplasty. A prospective, controlled, longitudinal study. *J Bone Joint Surg Am.* 1998 Oct;80(10):1447-58. PubMed PMID: 9801213. Epub 1998/11/04. eng.
73. Back DL, Dalziel R, Young D, Shimmin A. Early results of primary Birmingham hip resurfacings. *Journal of Bone & Joint Surgery, British Volume.* 2005;87-B(3):324-9.
74. Brodner W, Bitzan P, Meisinger V, Kaider A, Gottsauner-Wolf F, Kotz R. Serum cobalt levels after metal-on-metal total hip arthroplasty. *J Bone Joint Surg Am.* 2003 Nov;85-A(11):2168-73. PubMed PMID: 14630848. Epub 2003/11/25. eng.
75. Clarke MT, Lee PTH, Arora A, Villar RN. Levels of metal ions after small- and large-diameter metal-on-metal hip arthroplasty. *Journal of Bone & Joint Surgery, British Volume.* 2003;85-B(6):913-7.
76. Savarino L, Greco M, Cenni E, Cavasinni L, Rotini R, Baldini N, et al. Differences in ion release after ceramic-on-ceramic and metal-on-metal total hip replacement. *Journal of Bone & Joint Surgery, British Volume.* 2006;88-B(4):472-6.
77. Engh C, MacDonald S, Sritulanondha S, Thompson A, Naudie D, Engh C. 2008 John Charnley Award: Metal Ion Levels After Metal-on-Metal Total Hip Arthroplasty: &i>A Randomized Trial</i>. *Clinical Orthopaedics and Related Research®.* 2009;467(1):101-11.
78. Rasquinha VJ, Ranawat CS, Weiskopf J, Rodriguez JA, Skipor AK, Jacobs JJ. Serum metal levels and bearing surfaces in total hip arthroplasty. *J Arthroplasty.* 2006 Sep;21(6 Suppl 2):47-52. PubMed PMID: 16950061. Epub 2006/09/05. eng.
79. Kwon YM, Xia Z, Glyn-Jones S, Beard D, Gill HS, Murray DW. Dose-dependent cytotoxicity of clinically relevant cobalt nanoparticles and ions on macrophages in vitro. *Biomed Mater.* 2009 Apr;4(2):025018. PubMed PMID: 19349653. Epub 2009/04/08. eng.
80. Horowitz SM, Gonzales JB. Inflammatory Response to Implant Particulates in a Macrophage/Osteoblast Coculture Model. *Calcified Tissue International.* 1996;59(5):392-6.
81. Fritz EA, Jacobs JJ, Glant TT, Roebuck KA. Chemokine IL-8 induction by particulate wear debris in osteoblasts is mediated by NF-κB. *Journal of Orthopaedic Research.* 2005;23(6):1249-57.

82. Fritz EA, Glant TT, Vermes C, Jacobs JJ, Roebuck KA. Chemokine gene activation in human bone marrow-derived osteoblasts following exposure to particulate wear debris. *Journal of Biomedical Materials Research Part A*. 2006;77A(1):192-201.
83. Coleman RF, Herrington J, Scales JT. Concentration of wear products in hair, blood, and urine after total hip replacement. *Br Med J*. 1973 Mar 3;1(5852):527-9. PubMed PMID: 4692678. Pubmed Central PMCID: 1588720. Epub 1973/03/03. eng.
84. Merritt K, Brown SA. Effects of Metal Particles and Ions on the Biological System. *Techniques in Orthopaedics*. 1993;8(4).
85. Jacobs JJ, Gilbert JL, Urban RM. Corrosion of metal orthopaedic implants. *J Bone Joint Surg Am*. 1998 Feb;80(2):268-82. PubMed PMID: 9486734. Epub 1998/03/05. eng.
86. Cobb AG, Schmalzreid TP. The clinical significance of metal ion release from cobalt-chromium metal-on-metal hip joint arthroplasty. *Proceedings of the Institution of Mechanical Engineers, Part H: Journal of Engineering in Medicine*. 2006;220(2):385-98.
87. Grigoris P, Roberts P, Panousis K, Bosch H. The evolution of hip resurfacing arthroplasty. *Orthop Clin North Am*. 2005 Apr;36(2):125-34, vii. PubMed PMID: 15833450. Epub 2005/04/19. eng.
88. Doorn PF, Campbell PA, Worrall J, Benya PD, McKellop HA, Amstutz HC. Metal wear particle characterization from metal on metal total hip replacements: Transmission electron microscopy study of periprosthetic tissues and isolated particles. *Journal of Biomedical Materials Research*. 1998;42(1):103-11.
89. Germain MA, Hatton A, Williams S, Matthews JB, Stone MH, Fisher J, et al. Comparison of the cytotoxicity of clinically relevant cobalt-chromium and alumina ceramic wear particles in vitro. *Biomaterials*. 2003 Feb;24(3):469-79. PubMed PMID: 12423602. Epub 2002/11/09. eng.
90. Dumbleton JH, Manley MT. Metal-on-Metal Total Hip Replacement: What Does the Literature Say? *The Journal of Arthroplasty*. 2005;20(2):174-88.
91. Lhotka C, Szekeres T, Steffan I, Zhuber K, Zweymüller K. Four-year study of cobalt and chromium blood levels in patients managed with two different metal-on-metal total hip replacements. *Journal of Orthopaedic Research*. 2003;21(2):189-95.

92. Milošev I, Pišot V, Campbell P. Serum levels of cobalt and chromium in patients with Sikomet metal-metal total hip replacements. *Journal of Orthopaedic Research*. 2005;23(3):526-35.
93. Bohler M, Kanz F, Schwarz B, Steffan I, Walter A, Plenk H, Jr., et al. Adverse tissue reactions to wear particles from Co-alloy articulations, increased by alumina-blasting particle contamination from cementless Ti-based total hip implants. A report of seven revisions with early failure. *J Bone Joint Surg Br*. 2002 Jan;84(1):128-36. PubMed PMID: 11837818. Epub 2002/02/12. eng.
94. Catelas I, Petit A, Zukor DJ, Antoniou J, Huk OL. TNF- α secretion and macrophage mortality induced by cobalt and chromium ions in vitro-Qualitative analysis of apoptosis. *Biomaterials*. 2003;24(3):383-91.
95. Catelas I, Petit A, Vali H, Fragiskatos C, Meilleur R, Zukor DJ, et al. Quantitative analysis of macrophage apoptosis vs. necrosis induced by cobalt and chromium ions in vitro. *Biomaterials*. 2005;26(15):2441-53.
96. Daou S, El Chemaly A, Christofilopoulos P, Bernard L, Hoffmeyer P, Demaurex N. The potential role of cobalt ions released from metal prosthesis on the inhibition of Hv1 proton channels and the decrease in *Staphylococcus epidermidis* killing by human neutrophils. *Biomaterials*. 2011 Mar;32(7):1769-77. PubMed PMID: 21138781. Epub 2010/12/09. eng.
97. Petit A, Mwale F, Zukor DJ, Catelas I, Antoniou J, Huk OL. Effect of cobalt and chromium ions on bcl-2, bax, caspase-3, and caspase-8 expression in human U937 macrophages. *Biomaterials*. 2004;25(11):2013-8.
98. Huk OL, Catelas I, Mwale F, Antoniou J, Zukor DJ, Petit A. Induction of apoptosis and necrosis by metal ions in vitro. *The Journal of Arthroplasty*. 2004;19(8, Supplement):84-7.
99. Vandana S, Ram S, Ilavazhagan M, Kumar GD, Banerjee PK. Comparative cytoprotective activity of vitamin C, E and beta-carotene against chromium induced oxidative stress in murine macrophages. *Biomed Pharmacother*. 60. France2006. p. 71-6.
100. Maezawa K, Nozawa M, Hirose T, Matsuda K, Yasuma M, Shitoto K, et al. Cobalt and chromium concentrations in patients with metal-on-metal and other cementless total hip arthroplasty. *Arch Orthop Trauma Surg*. 2002 Jun;122(5):283-7. PubMed PMID: 12070648. Epub 2002/06/19. eng.

101. Granchi D, Savarino L, Ciapetti G, Cenni E, Rotini R, Mieti M, et al. Immunological changes in patients with primary osteoarthritis of the hip after total joint replacement. *J Bone Joint Surg Br.* 2003 Jul;85(5):758-64. PubMed PMID: 12892206. Epub 2003/08/02. eng.
102. Hart AJ, Hester T, Sinclair K, Powell JJ, Goodship AE, Pele L, et al. The association between metal ions from hip resurfacing and reduced T-cell counts. *J Bone Joint Surg Br.* 2006 Apr;88(4):449-54. PubMed PMID: 16567777. Epub 2006/03/29. eng.
103. Ladon D, Doherty A, Newson R, Turner J, Bhamra M, Case CP. Changes in metal levels and chromosome aberrations in the peripheral blood of patients after metal-on-metal hip arthroplasty. *The Journal of Arthroplasty.* 2004;19(8, Supplement):78-83.
104. Hart AJ, Skinner JA, Winship P, Faria N, Kulinskaya E, Webster D, et al. Circulating levels of cobalt and chromium from metal-on-metal hip replacement are associated with CD8+ T-cell lymphopenia. *J Bone Joint Surg Br.* 2009 Jun;91(6):835-42. PubMed PMID: 19483243. Epub 2009/06/02. eng.
105. Campbell P, Ebramzadeh E, Nelson S, Takamura K, De Smet K, Amstutz HC. Histological features of pseudotumor-like tissues from metal-on-metal hips. *Clin Orthop Relat Res.* 2010 Sep;468(9):2321-7. PubMed PMID: 20458645. Pubmed Central PMCID: 2914255. Epub 2010/05/12. eng.
106. Gruber FW, Bock A, Trattinig S, Lintner F, Ritschl P. Cystic lesion of the groin due to metallosis: a rare long-term complication of metal-on-metal total hip arthroplasty. *J Arthroplasty.* 2007 Sep;22(6):923-7. PubMed PMID: 17826287. Epub 2007/09/11. eng.
107. Boardman DR, Middleton FR, Kavanagh TG. A benign psoas mass following metal-on-metal resurfacing of the hip. *J Bone Joint Surg Br.* 2006 Mar;88(3):402-4. PubMed PMID: 16498023. Epub 2006/02/25. eng.
108. Bosker BH, Ettema HB, Boomsma MF, Kollen BJ, Maas M, Verheyen CC. High incidence of pseudotumour formation after large-diameter metal-on-metal total hip replacement: A prospective cohort study. *J Bone Joint Surg Br.* 2012 Jun;94(6):755-61. PubMed PMID: 22628588. Epub 2012/05/26. eng.
109. Ollivere B, Darrah C, Barker T, Nolan J, Porteous MJ. Early clinical failure of the Birmingham metal-on-metal hip resurfacing is associated with metallosis and soft-tissue necrosis. *J Bone Joint Surg Br.* 2009 Aug;91(8):1025-30. PubMed PMID: 19651828. Epub 2009/08/05. eng.

110. Leigh W, O'Grady P, Lawson EM, Hung NA, Theis JC, Matheson J. Pelvic pseudotumor: an unusual presentation of an extra-articular granuloma in a well-fixed total hip arthroplasty. *J Arthroplasty*. 2008 Sep;23(6):934-8. PubMed PMID: 18534517. Epub 2008/06/07. eng.
111. Svensson O, Mathiesen EB, Reinholt FP, Blomgren G. Formation of a fulminant soft-tissue pseudotumor after uncemented hip arthroplasty. A case report. *J Bone Joint Surg Am*. 1988 Sep;70(8):1238-42. PubMed PMID: 3417709. Epub 1988/09/01. eng.
112. Murray DW. Pseudotumour following hip resurfacing. Early intervention in the hip and knee. . *The Great Debate*. London 2009.
113. Treacy RB, McBryde CW, Pynsent PB. Birmingham hip resurfacing arthroplasty. A minimum follow-up of five years. *J Bone Joint Surg Br*. 2005 Feb;87(2):167-70. PubMed PMID: 15736736. Epub 2005/03/02. eng.
114. Grammatopolous G, Pandit H, Kwon YM, Gundle R, McLardy-Smith P, Beard DJ, et al. Hip resurfacings revised for inflammatory pseudotumour have a poor outcome. *J Bone Joint Surg Br*. 91. England 2009. p. 1019-24.
115. Xia Z, Triffitt JT. A review on macrophage responses to biomaterials. *Biomed Mater*. 2006 Mar;1(1):R1-9. PubMed PMID: 18458376. Epub 2008/05/07. eng.
116. Hallab N, J. Jacobs J, Black J. Hypersensitivity to metallic biomaterials: a review of leukocyte migration inhibition assays. *Biomaterials*. 2000;21(13):1301-14.
117. Hanssen AD, Rand JA. Evaluation and treatment of infection at the site of a total hip or knee arthroplasty. *Instr Course Lect*. 1999;48:111-22. PubMed PMID: 10098033. Epub 1999/03/31. eng.
118. Lentino JR. Prosthetic joint infections: bane of orthopedists, challenge for infectious disease specialists. *Clin Infect Dis*. 2003 May 1;36(9):1157-61. PubMed PMID: 12715311. Epub 2003/04/26. eng.
119. Liu YK, Xu H, Liu F, Tao R, Yin J. Effects of serum cobalt ion concentration on the liver, kidney and heart in mice. *Orthop Surg*. 2010 May;2(2):134-40. PubMed PMID: 22009928. Epub 2010/05/01. eng.
120. Brock T, Stopford W. Bioaccessibility of metals in human health risk assessment: evaluating risk from exposure to cobalt compounds. *J Environ Monit*. 2003 Aug;5(4):71N-6N. PubMed PMID: 12948221. Epub 2003/09/02. eng.

121. Darbre PD. Metalloestrogens: an emerging class of inorganic xenoestrogens with potential to add to the oestrogenic burden of the human breast. *J Appl Toxicol.* 2006 May-Jun;26(3):191-7. PubMed PMID: 16489580. Epub 2006/02/21. eng.
122. Keegan GM, Learmonth ID, Case CP. Orthopaedic metals and their potential toxicity in the arthroplasty patient: A review of current knowledge and future strategies. *J Bone Joint Surg Br.* 2007 May;89(5):567-73. PubMed PMID: 17540737. Epub 2007/06/02. eng.
123. Ani M, Moshtaghie AA. The effect of chromium on parameters related to iron metabolism. *Biol Trace Elem Res.* 1992 Jan-Mar;32:57-64. PubMed PMID: 1375087. Epub 1992/01/01. eng.
124. Kurosaki K, Nakamura T, Mukai T, Endo T. Unusual findings in a fatal case of poisoning with chromate compounds. *Forensic science international.* 1995;75(1):57-65.
125. Oliveira H, Santos TM, Ramalho-Santos J, de Lourdes Pereira M. Histopathological Effects of Hexavalent Chromium in Mouse Kidney. *Bulletin of Environmental Contamination and Toxicology.* 2006;76(6):977-83.
126. Aruldas MM, Subramanian S, Sekar P, Vengatesh G, Chandrahasan G, Govindarajulu P, et al. Chronic chromium exposure-induced changes in testicular histoarchitecture are associated with oxidative stress: study in a non-human primate (*Macaca radiata* Geoffroy). *Hum Reprod.* 2005 Oct;20(10):2801-13. PubMed PMID: 15980013. Epub 2005/06/28. eng.
127. Nemery B. Metal toxicity and the respiratory tract. *Eur Respir J.* 1990 Feb;3(2):202-19. PubMed PMID: 2178966. Epub 1990/02/01. eng.
128. Kanojia RK, Junaid M, Murthy RC. Embryo and fetotoxicity of hexavalent chromium: a long-term study. *Toxicology Letters.* 1998;95(3):165-72.
129. Morin Y, Tetu A, Mercier G. Cobalt cardiomyopathy: clinical aspects. *Br Heart J.* 1971;33:Suppl:175-8. PubMed PMID: 5280148. Pubmed Central PMCID: 503291. Epub 1971/01/01. eng.
130. Mercier G, Patry G. Quebec beer-drinkers' cardiomyopathy: clinical signs and symptoms. *Can Med Assoc J.* 1967 Oct 7;97(15):884-8. PubMed PMID: 6051257. Pubmed Central PMCID: 1923407. Epub 1967/10/07. eng.
131. Alexander CS. Cobalt-beer cardiomyopathy. A clinical and pathologic study of twenty-eight cases. *Am J Med.* 1972

- Oct;53(4):395-417. PubMed PMID: 4263183. Epub 1972/10/01. eng.
132. Busse B, Hahn M, Niecke M, Jobke B, Puschel K, Delling G, et al. Allocation of nonbirefringent wear debris: darkfield illumination associated with PIXE microanalysis reveals cobalt deposition in mineralized bone matrix adjacent to CoCr implants. *J Biomed Mater Res A*. 2008 Nov;87(2):536-45. PubMed PMID: 18186044. Epub 2008/01/11. eng.
133. Nakashima Y, Sun DH, Maloney WJ, Goodman SB, Schurman DJ, Smith RL. Induction of matrix metalloproteinase expression in human macrophages by orthopaedic particulate debris in vitro. *J Bone Joint Surg Br*. 1998 Jul;80(4):694-700. PubMed PMID: 9699840. Epub 1998/08/12. eng.
134. Haynes DR, Rogers SD, Hay S, Pearcy MJ, Howie DW. The differences in toxicity and release of bone-resorbing mediators induced by titanium and cobalt-chromium-alloy wear particles. *J Bone Joint Surg Am*. 1993 Jun;75(6):825-34. PubMed PMID: 8314823. Epub 1993/06/01. eng.
135. Haynes DR, Hay SJ, Rogers SD, Ohta S, Howie DW, Graves SE. Regulation of bone cells by particle-activated mononuclear phagocytes. *J Bone Joint Surg Br*. 1997 Nov;79(6):988-94. PubMed PMID: 9393919. Epub 1997/12/11. eng.
136. Caetano-Lopes J, Canhao H, Fonseca JE. Osteoblasts and bone formation. *Acta Reumatol Port*. 2007 Apr-Jun;32(2):103-10. PubMed PMID: 17572649. Epub 2007/06/19. eng.
137. Ducy P, Schinke T, Karsenty G. The Osteoblast: A Sophisticated Fibroblast under Central Surveillance. *Science*. 2000;289(5484):1501-4.
138. Seeman E. Osteocytes—martyrs for integrity of bone strength. *Osteoporosis International*. 2006;17(10):1443-8.
139. Gori F, Hofbauer LC, Dunstan CR, Spelsberg TC, Khosla S, Riggs BL. The expression of osteoprotegerin and RANK ligand and the support of osteoclast formation by stromal-osteoblast lineage cells is developmentally regulated. *Endocrinology*. 2000 Dec;141(12):4768-76. PubMed PMID: 11108292. Epub 2000/12/07. eng.
140. Krane SM. Identifying genes that regulate bone remodeling as potential therapeutic targets. *The Journal of Experimental Medicine*. 2005;201(6):841-3.

141. Mackie EJ. Osteoblasts: novel roles in orchestration of skeletal architecture. *The International Journal of Biochemistry & Cell Biology*. 2003;35(9):1301-5.
142. Anissian L, Stark A, Dahlstrand H, Granberg B, Good V, Bucht E. Cobalt ions influence proliferation and function of human osteoblast-like cells. *Acta Orthop Scand*. 2002 Jun;73(3):369-74. PubMed PMID: 12143988. Epub 2002/07/30. eng.
143. Hallab NJ, Vermes C, Messina C, Roebuck KA, Glant TT, Jacobs JJ. Concentration- and composition-dependent effects of metal ions on human MG-63 osteoblasts. *J Biomed Mater Res*. 2002 Jun 5;60(3):420-33. PubMed PMID: 11920666. Epub 2002/03/29. eng.
144. Sun ZL, Wataha JC, Hanks CT. Effects of metal ions on osteoblast-like cell metabolism and differentiation. *J Biomed Mater Res*. 1997 Jan;34(1):29-37. PubMed PMID: 8978650. Epub 1997/01/01. eng.
145. Wang JY, Wicklund BH, Gustilo RB, Tsukayama DT. Prosthetic Metals Interfere With the Functions of Human Osteoblast Cells In Vitro. *Clinical Orthopaedics and Related Research*. 1997;339.
146. Nichols KG, Puleo DA. Effect of metal ions on the formation and function of osteoclastic cells in vitro. *J Biomed Mater Res*. 1997 May;35(2):265-71. PubMed PMID: 9135175. Epub 1997/05/01. eng.
147. Study RE, Breakefield XO, Bartfai T, Greengard P. Voltage-sensitive calcium channels regulate guanosine 3',5'-cyclic monophosphate levels in neuroblastoma cells. *Proc Natl Acad Sci U S A*. 1978 Dec;75(12):6295-9. PubMed PMID: 216020. Pubmed Central PMCID: 393168. Epub 1978/12/01. eng.
148. Moger WH. Effects of the calcium-channel blockers cobalt, verapamil, and D600 on Leydig cell steroidogenesis. *Biol Reprod*. 1983 Apr;28(3):528-35. PubMed PMID: 6303461. Epub 1983/04/01. eng.
149. Shibuya I, Douglas WW. Calcium channels in rat melanotrophs are permeable to manganese, cobalt, cadmium, and lanthanum, but not to nickel: evidence provided by fluorescence changes in fura-2-loaded cells. *Endocrinology*. 1992 Oct;131(4):1936-41. PubMed PMID: 1327724. Epub 1992/10/01. eng.
150. Puopolo M, Raviola E, Bean BP. Roles of subthreshold calcium current and sodium current in spontaneous firing of mouse midbrain dopamine neurons. *J Neurosci*. 2007 Jan 17;27(3):645-56. PubMed PMID: 17234596. Epub 2007/01/20. eng.

151. Grygorczyk C, Grygorczyk R, Ferrier J. Osteoblastic cells have L-type calcium channels. *Bone Miner.* 1989 Sep;7(2):137-48. PubMed PMID: 2478237. Epub 1989/09/01. eng.
152. Dolphin AC. *Calcium Channel Diversity.* eLS: John Wiley & Sons, Ltd; 2001.
153. Randall AD, Tsien RW. Contrasting biophysical and pharmacological properties of T-type and R-type calcium channels. *Neuropharmacology.* 1997;36(7):879-93.
154. Duncan RL, Akanbi KA, Farach-Carson MC. Calcium signals and calcium channels in osteoblastic cells. *Semin Nephrol.* 1998 Mar;18(2):178-90. PubMed PMID: 9541272. Epub 1998/04/16. eng.
155. Thibault O, Hadley R, Landfield PW. Elevated postsynaptic $[Ca^{2+}]_i$ and L-type calcium channel activity in aged hippocampal neurons: relationship to impaired synaptic plasticity. *J Neurosci.* 2001 Dec 15;21(24):9744-56. PubMed PMID: 11739583. Epub 2001/12/12. eng.
156. Durante P, Cardenas CG, Whittaker JA, Kitai ST, Scroggs RS. Low-threshold L-type calcium channels in rat dopamine neurons. *J Neurophysiol.* 2004 Mar;91(3):1450-4. PubMed PMID: 14645383. Epub 2003/12/03. eng.
157. Davidoff AJ, Maki TM, Ellingsen O, Marsh JD. Expression of calcium channels in adult cardiac myocytes is regulated by calcium. *J Mol Cell Cardiol.* 1997 Jul;29(7):1791-803. PubMed PMID: 9236134. Epub 1997/07/01. eng.
158. White JA, McKinney BC, John MC, Powers PA, Kamp TJ, Murphy GG. Conditional forebrain deletion of the L-type calcium channel $Ca_V 1.2$ disrupts remote spatial memories in mice. *Learn Mem.* 2008 Jan;15(1):1-5. PubMed PMID: 18174367. Epub 2008/01/05. eng.
159. Pazzaglia PJ, Post RM, Ketter TA, Callahan AM, Marangell LB, Frye MA, et al. Nimodipine monotherapy and carbamazepine augmentation in patients with refractory recurrent affective illness. *J Clin Psychopharmacol.* 1998 Oct;18(5):404-13. PubMed PMID: 9790159. Epub 1998/10/28. eng.
160. Premkumar LS. Selective potentiation of L-type calcium channel currents by cocaine in cardiac myocytes. *Mol Pharmacol.* 1999 Dec;56(6):1138-42. PubMed PMID: 10570040. Epub 1999/11/26. eng.
161. Calin-Jageman I, Lee A. $Cav1$ L-type Ca^{2+} channel signaling complexes in neurons. *Journal of Neurochemistry.* 2008;105(3):573-83.

162. Monnier N, Procaccio V, Stieglitz P, Lunardi J. Malignant-hyperthermia susceptibility is associated with a mutation of the alpha 1-subunit of the human dihydropyridine-sensitive L-type voltage-dependent calcium-channel receptor in skeletal muscle. *Am J Hum Genet.* 1997 Jun;60(6):1316-25. PubMed PMID: 9199552. Pubmed Central PMCID: 1716149. Epub 1997/06/01. eng.
163. Walker LM, Publicover SJ, Preston MR, Said Ahmed MA, El Haj AJ. Calcium-channel activation and matrix protein upregulation in bone cells in response to mechanical strain. *J Cell Biochem.* 2000 Sep 14;79(4):648-61. PubMed PMID: 10996855. Epub 2000/09/21. eng.
164. Ryder KD, Duncan RL. Parathyroid hormone enhances fluid shear-induced $[Ca^{2+}]_i$ signaling in osteoblastic cells through activation of mechanosensitive and voltage-sensitive Ca^{2+} channels. *J Bone Miner Res.* 2001 Feb;16(2):240-8. PubMed PMID: 11204424. Epub 2001/02/24. eng.
165. Li J, Duncan RL, Burr DB, Turner CH. L-Type Calcium Channels Mediate Mechanically Induced Bone Formation In Vivo. *Journal of Bone and Mineral Research.* 2002;17(10):1795-800.
166. Jorgensen NR, Henriksen Z, Sorensen OH, Eriksen EF, Civitelli R, Steinberg TH. Intercellular calcium signaling occurs between human osteoblasts and osteoclasts and requires activation of osteoclast P2X7 receptors. *J Biol Chem.* 2002 Mar 1;277(9):7574-80. PubMed PMID: 11756404. Epub 2002/01/05. eng.
167. Li J, Duncan RL, Burr DB, Gattone VH, Turner CH. Parathyroid hormone enhances mechanically induced bone formation, possibly involving L-type voltage-sensitive calcium channels. *Endocrinology.* 2003 Apr;144(4):1226-33. PubMed PMID: 12639904. Epub 2003/03/18. eng.
168. Nishiya Y, Kosaka N, Uchii M, Sugimoto S. A potent 1,4-dihydropyridine L-type calcium channel blocker, benidipine, promotes osteoblast differentiation. *Calcif Tissue Int.* 2002 Jan;70(1):30-9. PubMed PMID: 11907705. Epub 2002/03/22. eng.
169. Jorgensen NR. Short-range intercellular calcium signaling in bone. *APMIS Suppl.* 2005 (118):5-36. PubMed PMID: 16279161. Epub 2005/11/11. eng.
170. Bergh JJ, Shao Y, Puente E, Duncan RL, Farach-Carson MC. Osteoblast Ca^{2+} permeability and voltage-sensitive Ca^{2+} channel expression is temporally regulated by 1,25-dihydroxyvitamin D3. *American Journal of Physiology - Cell Physiology.* 2006;290(3):C822-C31.

171. Jorgensen L, Engstad T, Jacobsen BK. Bone mineral density in acute stroke patients: low bone mineral density may predict first stroke in women. *Stroke*. 2001 Jan;32(1):47-51. PubMed PMID: 11136913. Epub 2001/01/04. eng.
172. Nesti LJ, Caterson EJ, Wang M, Chang R, Chapovsky F, Hoek JB, et al. TGF-beta1 calcium signaling increases alpha5 integrin expression in osteoblasts. *J Orthop Res*. 2002 Sep;20(5):1042-9. PubMed PMID: 12382972. Epub 2002/10/18. eng.
173. www.drugs.com/pro/verapamil.html 2012 [12 July 2012].
174. <http://www.drugs.com/pro/nifedipine-extended-release-tablets.html> 2012 [12 July 2012].
175. Sakai K, Mohtai M, Iwamoto Y. Fluid shear stress increases transforming growth factor beta 1 expression in human osteoblast-like cells: modulation by cation channel blockades. *Calcif Tissue Int*. 1998 Dec;63(6):515-20. PubMed PMID: 9817947. Epub 1998/11/18. eng.
176. Yamaguchi DT, Hahn TJ, Iida-Klein A, Kleeman CR, Muallem S. Parathyroid hormone-activated calcium channels in an osteoblast-like clonal osteosarcoma cell line. cAMP-dependent and cAMP-independent calcium channels. *J Biol Chem*. 1987 Jun 5;262(16):7711-8. PubMed PMID: 2438281. Epub 1987/06/05. eng.
177. Zijlstra WP, Bulstra SK, van Raay JJ, van Leeuwen BM, Kuijer R. Cobalt and chromium ions reduce human osteoblast-like cell activity in vitro, reduce the OPG to RANKL ratio, and induce oxidative stress. *J Orthop Res*. 2012 May;30(5):740-7. PubMed PMID: 22025323. Epub 2011/10/26. eng.
178. Borenfreund E, Puerner JA. Toxicity determined in vitro by morphological alterations and neutral red absorption. *Toxicol Lett*. 1985 Feb-Mar;24(2-3):119-24. PubMed PMID: 3983963. Epub 1985/02/01. eng.
179. GM. C. *The Cell: A Molecular Approach*. Available from: <http://www.ncbi.nlm.nih.gov/books/NBK9961/July> 2012: Sinauer Associates; 2000. 2nd edition. :[
180. Lanone S, Rogerieux F, Geys J, Dupont A, Maillot-Marechal E, Boczkowski J, et al. Comparative toxicity of 24 manufactured nanoparticles in human alveolar epithelial and macrophage cell lines. *Part Fibre Toxicol*. 6. England2009. p. 14.
181. Riccardi C, Nicoletti I. Analysis of apoptosis by propidium iodide staining and flow cytometry. *Nat Protoc*. 1. England2006. p. 1458-61.

182. Roe MW, Lemasters JJ, Herman B. Assessment of Fura-2 for measurements of cytosolic free calcium. *Cell Calcium*. 1990;11(2-3):63-73.
183. Chi C-C, Huang C-C, Chien J-M, Chu S-T, Chen W-C, Chang H-T, et al. L-type Ca²⁺ channel opener BayK 8644-induced Ca²⁺ influx and Ca²⁺ release in human oral cancer cells (OC2). *Drug Development Research*. 2008;69(8):508-13.
184. Guggino SE, Lajeunesse D, Wagner JA, Snyder SH. Bone remodeling signaled by a dihydropyridine- and phenylalkylamine-sensitive calcium channel. *Proc Natl Acad Sci U S A*. 1989 Apr;86(8):2957-60. PubMed PMID: 2468165. Pubmed Central PMCID: 287039. Epub 1989/04/01. eng.
185. Nawrath H, Raschack M. Effects of (-)-desmethoxyverapamil on heart and vascular smooth muscle. *J Pharmacol Exp Ther*. 1987 Sep;242(3):1090-7. PubMed PMID: 3656109. Epub 1987/09/01. eng.
186. Boutin P, Christel P, Dorlot JM, Meunier A, de Roquancourt A, Blanquaert D, et al. The use of dense alumina-alumina ceramic combination in total hip replacement. *J Biomed Mater Res*. 1988 Dec;22(12):1203-32. PubMed PMID: 3069846. Epub 1988/12/01. eng.
187. Mittelmeier H, Heisel J. Sixteen-years' experience with ceramic hip prostheses. *Clin Orthop Relat Res*. 1992 Sep(282):64-72. PubMed PMID: 1516330. Epub 1992/09/01. eng.
188. Mahoney OM, Dimon JH, 3rd. Unsatisfactory results with a ceramic total hip prosthesis. *J Bone Joint Surg Am*. 1990 Jun;72(5):663-71. PubMed PMID: 2355027. Epub 1990/06/01. eng.
189. Wirganowicz PZ, Thomas BJ. Massive osteolysis after ceramic on ceramic total hip arthroplasty. A case report. *Clin Orthop Relat Res*. 1997 May(338):100-4. PubMed PMID: 9170369. Epub 1997/05/01. eng.
190. Tsaousi A, Jones E, Case CP. The in vitro genotoxicity of orthopaedic ceramic (Al₂O₃) and metal (CoCr alloy) particles. *Mutation Research/Genetic Toxicology and Environmental Mutagenesis*. 2010;697(1-2):1-9.
191. Schmalzried TP, Callaghan JJ. Wear in total hip and knee replacements. *J Bone Joint Surg Am*. 1999 Jan;81(1):115-36. PubMed PMID: 9973062. Epub 1999/02/11. eng.
192. Case CP, Langkamer VG, Howell RT, Webb J, Standen G, Palmer M, et al. Preliminary observations on possible premalignant changes

in bone marrow adjacent to worn total hip arthroplasty implants. Clin Orthop Relat Res. 1996 Aug(329 Suppl):S269-79. PubMed PMID: 8769341. Epub 1996/08/01. eng.

193. Hummer CD, 3rd, Rothman RH, Hozack WJ. Catastrophic failure of modular zirconia-ceramic femoral head components after total hip arthroplasty. J Arthroplasty. 10. United States1995. p. 848-50.

194. Jarrett CA, Ranawat AS, Bruzzone M, Blum YC, Rodriguez JA, Ranawat CS. The squeaking hip: a phenomenon of ceramic-on-ceramic total hip arthroplasty. J Bone Joint Surg Am. 91. United States2009. p. 1344-9.

195. Park YS, Hwang SK, Choy WS, Kim YS, Moon YW, Lim SJ. Ceramic failure after total hip arthroplasty with an alumina-on-alumina bearing. J Bone Joint Surg Am. 88. United States2006. p. 780-7.

196. Hallam P, Haddad F, Cobb J. Pain in the well-fixed, aseptic titanium hip replacement. The role of corrosion. J Bone Joint Surg Br. 2004 Jan;86(1):27-30. PubMed PMID: 14765860. Epub 2004/02/10. eng.

197. Akbar M, Brewer JM, Grant MH. Effect of chromium and cobalt ions on primary human lymphocytes in vitro. J Immunotoxicol. 2011 Jun;8(2):140-9. PubMed PMID: 21446789. Epub 2011/03/31. eng.

198. Davies DG, Marques CN. A fatty acid messenger is responsible for inducing dispersion in microbial biofilms. J Bacteriol. 191. United States2009. p. 1393-403.

199. Harro JM, Peters BM, O'May GA, Archer N, Kerns P, Prabhakara R, et al. Vaccine development in Staphylococcus aureus: taking the biofilm phenotype into consideration. FEMS Immunol Med Microbiol. 59. England2010. p. 306-23.